

This is a repository copy of *Non-homogeneous Rapid Distortion Theory on transversely sheared mean flows*.

White Rose Research Online URL for this paper:

<https://eprints.whiterose.ac.uk/id/eprint/214210/>

Version: Accepted Version

Article:

Goldstein, Marvin, Koshuriyan, Zamir and Leib, Stewart J. (2013) Non-homogeneous Rapid Distortion Theory on transversely sheared mean flows. *Journal of Fluid Mechanics*. pp. 532-569. ISSN: 1469-7645

<https://doi.org/10.1017/jfm.2013.518>

Reuse

Items deposited in White Rose Research Online are protected by copyright, with all rights reserved unless indicated otherwise. They may be downloaded and/or printed for private study, or other acts as permitted by national copyright laws. The publisher or other rights holders may allow further reproduction and re-use of the full text version. This is indicated by the licence information on the White Rose Research Online record for the item.

Takedown

If you consider content in White Rose Research Online to be in breach of UK law, please notify us by emailing eprints@whiterose.ac.uk including the URL of the record and the reason for the withdrawal request.

Non-homogeneous Rapid Distortion Theory on transversely sheared mean flows

M. E. Goldstein¹, M. Z. Afsar¹ & S. J. Leib²

¹National Aeronautics and Space Administration, Glenn Research Centre, Cleveland OH 44135, USA

²Ohio Aerospace Institute, Cleveland, OH 44142 USA

This paper is concerned with the small amplitude unsteady motion of an inviscid non-heat conducting compressible fluid on a transversely sheared mean flow. It extends previous analyses (Goldstein, 1978b & 1979a) which show that the hydrodynamic component of the motion is determined by two arbitrary convected quantities in the absence of solid surfaces and hydrodynamic instabilities. These results can be used to specify appropriate upstream boundary conditions for unsteady surface interaction problems on transversely sheared mean flows in the same way that the vortical component of the Kovasznay (1953) decomposition is used to specify these conditions for surface interaction problems on uniform mean flows. But unlike Kovasznay's (1953) result the arbitrary convected quantities no longer bear a simple relation to the physical variables. A major purpose of this paper is to complete the formalism developed in Goldstein (1978b & 1979a) by obtaining the necessary relations between these quantities and the measurable flow variables. The results are important because they enable the complete extension of Non-homogeneous Rapid Distortion Theory to transversely sheared mean flows.

Another purpose of the paper is to derive a generalization of the famous Ffowcs Williams and Hall (1970) formula for the sound produced by the interaction of turbulence with an edge that is frequently used as a starting point for predicting sound generation by turbulence/solid surface interactions. We illustrate the utility of this result by using it to calculate the sound radiation produced by the interaction of a two-dimensional jet with the downstream edge of a flat plate.

1. Introduction

The small amplitude motion of an inviscid non-heat conducting compressible fluid is governed by the Linearized Euler Equations, i.e., the Euler equations linearized about an arbitrary, usually steady, solution to those equations— customarily referred to as the base flow. The simplest case occurs when the base flow is completely uniform. In a now classical paper, Kovasznay (1953) showed that the unsteady isentropic motion on this flow can be decomposed into the sum of a purely vortical disturbance that has no pressure fluctuations and an irrotational disturbance that carries the pressure fluctuations. The latter satisfies a second-order wave equation when the flow is compressible and should, as argued by Möhring (1976), either decay or propagate relative to the base flow. It can, therefore be associated with the acoustic component of the motion on these flows. The former, which moves downstream with the mean flow, i.e. it is a purely convected quantity, can be associated with the remaining, hydrodynamic, component of the motion. Any convected velocity field will satisfy the linearized momentum equation for this flow, but continuity only allows two of its components to be arbitrary. These two quantities can then be independently specified as steady state boundary conditions for unsteady surface interaction problems. This makes the Kovasznay decomposition particularly useful for analyzing the interaction of turbulence (which corresponds to the hydrodynamic component of the motion) with surfaces embedded in uniform mean flows (Sears, 1941), or in flows that become uniform in the upstream region (Hunt, 1973; Goldstein, 1978a, 1979b). It is worth noting, however, that the

Kovaszny decomposition is not unique because there are irrotational (homogeneous) solutions that carry no pressure fluctuations. There have been many attempts to extend these ideas to non-uniform base flows, but the situation is considerably more complicated when the entire base flow is non-uniform.

The simplest case occurs when the base flow U is incompressible and the mean shear is uniform i.e., $U = \gamma y_2$ where γ is a constant and y_1, y_2, y_3 are Cartesian coordinates, with y_1 being in the mean flow direction. Then the two-dimensional small amplitude motion is determined by the linearized incompressible vorticity equation $(\partial/\partial\tau + U\partial/\partial y_1)\omega_3 = 0$, where τ denotes the time and ω_3 denotes the two-dimensional vorticity perturbation. Orr (1907, see also Drazin & Reid, 1981, pp. 147-151) pointed out that this equation, or equivalently the two-dimensional Rayleigh equation

$$\frac{\partial}{\partial y_1} \left(\frac{\partial}{\partial \tau} + U \frac{\partial}{\partial y_1} \right) \omega_3 = \left(\frac{\partial}{\partial \tau} + U \frac{\partial}{\partial y_1} \right) \left(\frac{\partial^2}{\partial y_1^2} + \frac{\partial^2}{\partial y_2^2} \right) v'_2 = 0, \quad (1.1)$$

which determine and the unsteady transverse velocity perturbation $v'_2(y_2, \tau)$ can be integrated to obtain

$$\left(\frac{\partial^2}{\partial y_1^2} + \frac{\partial^2}{\partial y_2^2} \right) v'_2 = \frac{\partial}{\partial y_1} \omega_c \left(\tau - \frac{y_1}{\gamma y_2}, y_2 \right), \quad (1.2)$$

where the imposed transverse vorticity perturbation ω_c can be an arbitrary function of its arguments. Orr (1907) obtained an analytic solution to an initial value problem associated with this equation and used it to study the development of the velocity and pressure fluctuations starting from some initial state. But (1.2) can also be formulated as a steady-state (i.e. time-stationary) boundary value problem whose formal solution is given by

$$v'_2(\mathbf{x}, t) = \frac{\partial}{\partial x_1} \int_{-T}^T \int g_0(\mathbf{x}, t | \mathbf{y}, \tau) \omega_c \left(\tau - \frac{y_1}{\gamma y_2}, y_2 \right) dy d\tau, \quad (1.3)$$

where $\mathbf{x} = \{x_1, x_2\}$, $\mathbf{y} = \{y_1, y_2\}$ denote the two-dimensional Cartesian coordinates, the inner integration is over the entire $y_1 - y_2$ plane, T denotes a large time interval and g_0 denotes a two dimensional Poisson's equation Green's function that satisfies appropriate outgoing wave boundary conditions (Morse & Feshbach, 1953, p. 798).

Equation(1.2), which bears some relation to the so-called continuous spectrum, was extended to three-dimensional compressible motions on general planar compressible shear flows by Goldstein (1978 b, 1979 a: hereafter referred to as G78 & G79, respectively)--who showed how their more general results can be used to formulate surface interaction problems that are relevant to aircraft noise prediction. The G78 & G79 results are a natural generalization of the vortical solution in the Kovaszny (1953) decomposition in that they involve two arbitrary convected quantities, but neither of them can be associated with a single component of the vorticity.

Rapid Distortion Theory (RDT) uses linear analysis to study the interaction of turbulence with solid surfaces. It applies whenever the turbulence intensity is small and the time scale for the interaction is short compared to the decay time of the turbulent eddies (Hunt, 1973; Goldstein, 1984). Most of the

modern (i.e., non-homogeneous) RDT is concerned with small-amplitude vortical motion on potential flows that originate from a completely uniform upstream flow (Sagaut & Cambon, 2008; Hunt, 1973, 1977; Goldstein, 1978a, 1979 b; An excellent review of the status of non-homogeneous RDT as of 1990 can be found in Hunt & Carruthers, 1990). However, very little has been done on non-homogeneous RDT on transversely sheared mean flows or, more generally, sheared mean flows that originate from transversely sheared mean flows in the upstream region --presumably because of the difficulty in specifying upstream boundary conditions that can be controlled by the experimentalist .

In this paper, we consider the small-amplitude motion of an inviscid non-heat-conducting compressible fluid on a general transversely sheared mean flow with the aim of providing upstream boundary conditions that can be used to extend non-homogeneous RDT to flows of this type. The general formulas derived in section 2 of this paper show that the bounded solutions to the linearized Euler equations that govern the small amplitude motion on a transversely sheared mean flow involve two purely convected quantities that can be arbitrarily specified as input conditions. In the absence of scattering surfaces and other external sources the resulting flow consists entirely of subsonically propagating disturbances, which cannot radiate to the far field when the base flow is subsonic and unbounded (Goldstein, 2005 & 2009). This can easily be verified in any particular case by working out the relevant far field expansion. It is therefore appropriate to identify the unsteady flow produced by these convected quantities with the hydrodynamic component of the motion and use them to represent the upstream turbulence in the RDT formulation of surface interaction problems on this type of flow. But these quantities are not related to the physically measurable variables in any simple fashion. The required relations are obtained by considering the doubly infinite flow that would exist in the absence of any scattering inhomogeneities. This flow can be bounded or unbounded in the transverse direction, but must be completely homogeneous in the streamwise direction, which means that it cannot produce any significant change in the turbulence in that direction. It can be interpreted as the undisturbed flow that would exist upstream of any sudden surface interactions that occur in the flow. The two arbitrary convected quantities that appear in the general linearized Euler equation solutions derived in section 2 are then fixed by relating them to the physical variables on a flow of this type. This means that the input disturbances for the RDT problem are taken to be the bounded hydrodynamic disturbances (also referred to as “gust solutions”) on this streamwise homogeneous flow.

The paper begins by using a newly discovered relation between the G78 & G79 analysis and the Rayleigh equation Green’s function to extend that analysis in a number of important ways. The results allow us to use the Rayleigh operator Green’s function to write down a formal solution to the complete inhomogeneous RDT problem including a very simple formula for the unsteady pressure (equation (2.18) below) which generalizes the famous Ffowcs Williams and Hall (1970) equation (equation 6 in their paper) for the scattering of sound by a half plane. The latter has frequently been used as the starting point for analyses of solid surface interactions (most recently by Cavalieri, Jordan and Gervais, 2012), which are now of considerable interest because of their relevance to understanding and predicting the noise produced by the complex installations effects in current and future aircraft configurations. A major difference between the RDT approach and the Ffowcs Williams and Hall (1970) approach is that the former explicitly accounts for the mean flow interaction effects—which can become quite significant at the high Mach numbers of interest in aeronautical applications. Other important differences are that the Ffowcs Williams and Hall (1970) result cannot be used to predict the source convection velocity and does not account for trailing-edge vortex shedding-- both of which can

significantly affect trailing-edge noise directivity. The generalized formulas can (as described in Hunt & Curruthers, 1990) also be used to write down formal solutions to the complete RDT problems, which can potentially be used to develop or calibrate algebraic turbulence models.

As in G78 & G79 the unsteady motion is determined by two convected quantities that can be arbitrarily specified as boundary (or initial) conditions. But, as noted above, it is necessary to link these quantities to physical (preferably measurable) flow variables in order to relate the solution to conditions that can be controlled by an experimentalist. The necessary (explicit) relations for one of these quantities (which is usually of lesser importance because it does not appear in most applications of the theory) has already been given in Goldstein, Afsar and Leib (2013), while the relations for the other more important quantity, say $\tilde{\omega}_c$, are given in section 4 for an extensively studied class of transversely sheared mean flows. As noted above, the result is obtained by assuming that the relation between $\tilde{\omega}_c$ and the physical variables in the actual flow is the same as it would be for an idealized transversely sheared mean flow in which any bounding surfaces that may be present in the flow are doubly infinite in the streamwise direction (i.e., where the transverse boundary conditions are completely uniform in that direction). The solution relating the Fourier transform of the relevant physical variable to the Fourier transform of $\tilde{\omega}_c$ can then be inverted to obtain an explicit expression for the latter Fourier transform in terms of the former for an important class of mean flows.

Section 5 shows how this result can be used to calculate the $\tilde{\omega}_c$ spectrum, which turns out to be independent of the streamwise coordinate, and can consequently be related to streamwise-independent statistical quantities, even though the “gust solution” itself evolves in the streamwise direction. We are, therefore, able to use these results in sections 5, 6.4 and 6.5 to relate the statistical quantities, which are the main output of RDT to physically measurable statistical quantities that are independent of their streamwise location and , therefore, provide appropriate input boundary conditions for the streamwise inhomogeneous RDT problems. This is another important reason for using the convected quantities that appear in the RDT solutions to formulate surface interaction problems.

Section 6 illustrates the application of the generalized RDT formulation derived in this paper to surface interaction problems (i.e., problems involving the interaction of turbulence with solid surfaces and other non-uniformities) by using them to calculate the sound radiation produced by the interaction of a two-dimensional jet with the trailing edge of a flat plate—a problem which is currently of considerable interest because of its relevance to understanding noise production in future aircraft configurations. Comparisons with recent experiments conducted at the NASA Glenn Research Centre (Bridges & Brown 2013; Brown, 2012; Zaman, Brown & Bridges, 2013) are also presented in that section.

2. The basic formalism and comparison with the Ffowcs Williams and Hall and Orr results

We suppose that the flow is inviscid and non-heat conducting and assume an ideal gas so that the entropy is proportional to $\ln(p/\rho^\gamma)$ and the squared sound speed is $\gamma p/\rho$, where p denotes the pressure, ρ the density and γ the specific heat ratio. Then the inviscid pressure $p' = p - p_0$ and momentum flux

$$u_i \equiv \rho v'_i, \quad (2.1)$$

perturbations (where v'_i denotes the velocity perturbation) on a transversely sheared mean flow with pressure $p_0 = \text{constant}$, velocity $U(\mathbf{y}_T)$ and mean sound speed squared $c^2(\mathbf{y}_T)$ are governed by the linearized momentum and energy equations

$$\frac{D_0 u_i}{D\tau} + \delta_{ij} u_j \frac{\partial U}{\partial y_j} + \frac{\partial}{\partial y_i} p' = 0 \quad (2.2)$$

and

$$\frac{D_0 p'}{D\tau} + \frac{\partial}{\partial y_j} c^2 u_j = 0, \quad (2.3)$$

where $\mathbf{y}_T = \{y_2, y_3\}$, $\mathbf{y} = \{y_1, y_2, y_3\} = \{y_1, \mathbf{y}_T\}$ and $D_0 / D\tau \equiv \partial / \partial \tau + U \partial / \partial y_1$ denotes the convective derivative.

G79 points out that the momentum equation (2.2) will be identically satisfied for any function ϕ and any purely convected function $\mathfrak{G}(\tau - (y_1 / U), \mathbf{y}_T)$ when p' and u_i are determined by

$$p' = -\frac{D_0^3 \phi}{D\tau^3}, \quad (2.4)$$

$$u_i = \left(\delta_{ij} \frac{D_0}{D\tau} - \delta_{i1} \frac{\partial U}{\partial y_j} \right) \lambda_j + \varepsilon_{ijk} \frac{1}{c^2} \frac{\partial U}{\partial y_j} \frac{\partial}{\partial y_k} \mathfrak{G} \left(\tau - \frac{y_1}{U}, \mathbf{y}_T \right), \quad (2.5)$$

where δ_{ij} denotes the Kronecker delta, ε_{ijk} denotes the alternating tensor and

$$\lambda_j \equiv \frac{\partial}{\partial y_j} \frac{D_0 \phi}{D\tau} + 2 \frac{\partial U}{\partial y_j} \frac{\partial \phi}{\partial y_1} \quad (2.6)$$

denotes a kind of generalized particle displacement.

The arbitrary function ϕ can then be adjusted to ensure that the energy equation (2.3) is also satisfied by substituting (2.4)–(2.6) into (2.3) to obtain

$$\frac{D_0}{D\tau} \left[\frac{\partial}{\partial y_i} c^2 \left(\frac{\partial}{\partial y_i} \frac{D_0 \phi}{D\tau} + 2 \frac{\partial U}{\partial y_i} \frac{\partial \phi}{\partial y_1} \right) - \frac{D_0^3 \phi}{D\tau^3} \right] = 0, \quad (2.7)$$

which can then be integrated to obtain

$$L_a \phi = -\tilde{\omega}_c \left(\tau - \frac{y_1}{U}, \mathbf{y}_T \right), \quad (2.8)$$

where

$$L_a \equiv \frac{D_0^3}{D\tau^3} - \frac{\partial}{\partial y_i} c^2 \left(\frac{\partial}{\partial y_i} \frac{D_0}{D\tau} + 2 \frac{\partial U}{\partial y_i} \frac{\partial}{\partial y_1} \right). \quad (2.9)$$

It is well known that the momentum flux perturbation, u_i can be eliminated between (2.2) and (2.3) to show that the pressure fluctuation p' also satisfies Rayleigh's equation

$$L p' = 0, \quad (2.10)$$

where

$$L \equiv \frac{D_o}{D\tau} \left(\frac{\partial}{\partial y_i} c^2 \frac{\partial}{\partial y_i} - \frac{D_o^2}{D\tau^2} \right) - 2 \frac{\partial U}{\partial y_j} \frac{\partial}{\partial y_1} c^2 \frac{\partial}{\partial y_j} \quad (2.11)$$

denotes the usual Rayleigh operator. It is easy to show that L is adjoint to the operator L_a since, as can be readily verified,

$$\begin{aligned} vLu - uL_a v &= \frac{\partial}{\partial \tau} c^2 \left(u \frac{\partial}{\partial y_i} \frac{D_0 v}{D\tau} + 2u \frac{\partial U}{\partial y_i} \frac{\partial v}{\partial y_1} - \frac{\partial u}{\partial y_i} \frac{D_0 v}{D\tau} \right) \\ &+ \frac{D_o}{D\tau} \left(v \frac{\partial}{\partial y_i} c^2 \frac{\partial u}{\partial y_i} + \frac{D_0 u}{D\tau} \frac{D_o v}{D\tau} - u \frac{D_0^2 v}{D\tau^2} - v \frac{D_o^2 u}{D\tau^2} \right) - 2 \frac{\partial}{\partial y_1} \left(c^2 \frac{\partial U}{\partial y_j} v \frac{\partial u}{\partial y_j} \right) \end{aligned} \quad (2.12)$$

for any functions u, v . (Morse and Feshbach, 1953, p. 870, Tam and Auriault, 1998).

Let $g(\mathbf{y}, \tau | \mathbf{x}, t)$ satisfying

$$L g(\mathbf{y}, \tau | \mathbf{x}, t) = \delta(\mathbf{y} - \mathbf{x}) \delta(\tau - t) \quad (2.13)$$

be a Green's function for the Rayleigh operator L which exhibits incoming wave behaviour as $|\mathbf{y}| \rightarrow \infty$, where, as usual, the first two arguments denote the dependent variables and the second two denote the source variables. Since this function represents the solution to (2.13) at the point (\mathbf{y}, τ) due to a point source (or sink) at (\mathbf{x}, t) , it is reasonable to expect that it be related to its adjoint $g_a(\mathbf{x}, t | \mathbf{y}, \tau)$ by the usual reciprocity relation $g(\mathbf{y}, \tau | \mathbf{x}, t) = g_a(\mathbf{x}, t | \mathbf{y}, \tau)$ (Morse and Feshbach, 1953, Tam and Auriault, 1998). Then since $g_a(\mathbf{x}, t | \mathbf{y}, \tau)$, satisfies (2.8) with a delta function source term and, therefore, plays the role of the direct Greens function in the present context, we expect it to satisfy the causality condition $g_a(\mathbf{x}, t | \mathbf{y}, \tau) = 0$, for all $t < \tau$. The Green's function, $g(\mathbf{y}, \tau | \mathbf{x}, t)$, will then vanish for all finite \mathbf{y} as $\tau \rightarrow \infty$, since it vanishes for all $\tau > t$ by definition.

We also expect that the solution $\phi(\mathbf{x}, t)$ of (2.8) and its derivatives will vanish at the end points $x_1 \rightarrow \pm\infty$ for all finite t when $\tilde{\omega}_c$ is sufficiently compact—even when the base flow U is globally unstable because the signal generated at \mathbf{y}, τ cannot reach these locations when $t = T$ is finite, which means that $\phi(\mathbf{y}, \tau)$ should go to zero as $y_1 \rightarrow \pm\infty$ for all finite τ . An alternate justification for this

assertion can be found in Tam and Auriault (1998). And finally we assume that the initial conditions require that $\phi(\mathbf{y}, \tau)$ together with its derivatives vanish for all finite \mathbf{y} as $\tau \rightarrow -\infty$.

Letting v be the solution to (2.8) that satisfies these conditions, setting u equal to $g(\mathbf{y}, \tau | \mathbf{x}, t)$ in (2.12), and applying the divergence theorem now shows that

$$\begin{aligned} \phi(\mathbf{x}, t) = & - \int_{-T}^T \int_V g(\mathbf{y}, \tau | \mathbf{x}, t) \tilde{\omega}_c \left(\tau - \frac{y_1}{U(\mathbf{y}_T)}, \mathbf{y}_T \right) d\mathbf{y} d\tau \\ & + \int_{-T}^T \int_S \hat{n}_j c^2 \left[g(\mathbf{y}, \tau | \mathbf{x}, t) \lambda_j - \frac{\partial g(\mathbf{y}, \tau | \mathbf{x}, t)}{\partial y_j} \frac{D_0 \phi}{D\tau} \right] dS(\mathbf{y}) d\tau \end{aligned} \quad (2.14)$$

where T denotes a very large but finite time interval, V is a region of space bounded by cylindrical (i.e., parallel to the mean flow) surface(s) S that can be finite, semi-infinite or infinite in the streamwise direction and $\hat{\mathbf{n}} = \{\hat{n}_i\}$ is the unit outward-drawn normal to S . We have omitted terms that are negligibly small as $T \rightarrow \pm\infty$ and neglected the contribution from the end caps (as was done, for example, in Tam and Auriault, 1998). This formula expresses the solution to equation (2.8) in terms of the volume source distribution $\tilde{\omega}_c(\tau - y_1/U(\mathbf{y}_T), \mathbf{y}_T)$ and the values of ϕ on some arbitrary cylindrical surfaces S (some or all of which may be at infinity). The analysis is somewhat unconventional in that the direct Green's function g now plays the role of an adjoint Green's function for the solution ϕ .

The surface terms drop out when the surface S is at infinity, i.e. V is all space, and in the more general case, where the surface integrals do not vanish, equations (2.4) and (2.14) show that the pressure perturbation $p'(\mathbf{x}, t)$ is given by

$$\begin{aligned} p'(\mathbf{x}, t) = & \int_{-T}^T \int_V \frac{D_0^3 g(\mathbf{y}, \tau | \mathbf{x}, t)}{Dt^3} \tilde{\omega}_c \left(\tau - \frac{y_1}{U(\mathbf{y}_T)}, \mathbf{y}_T \right) d\mathbf{y} d\tau \\ & - \int_{-T}^T \int_S \left[\frac{D_0^3 g(\mathbf{y}, \tau | \mathbf{x}, t)}{Dt^3} (\hat{n}_j \lambda_j c^2) - \frac{D_0^3 \gamma(\mathbf{y}, \tau | \mathbf{x}, t)}{Dt^3} \frac{D_0^3 \phi}{D\tau^3} \right] dS(\mathbf{y}) d\tau, \end{aligned} \quad (2.15)$$

where we have integrated by parts and put

$$\frac{D_0^2 \gamma}{D\tau^2} \equiv c^2 \hat{n}_j \frac{\partial g(\mathbf{y}, \tau | \mathbf{x}, t)}{\partial y_j}. \quad (2.16)$$

Similar formulas can, of course, be written down for the momentum perturbation components $u_i(\mathbf{x}, t)$, which will, in general, depend on the second convected quantity \mathcal{Q} .

The surface integrals can frequently be eliminated by noting that the Green's function g is not uniquely determined by (2.13) and can be required to satisfy certain boundary conditions on the bounding surface S . We could, for example, require that

$$\frac{D_0^3 \gamma(\mathbf{y}, \tau | \mathbf{x}, t)}{Dt^3} = 0, \quad \text{for } \mathbf{y} \in S \quad (2.17)$$

and that $D_0^3 g(\mathbf{y}, \tau | \mathbf{x}, t) / Dt^3$ and $D_0^3 \gamma(\mathbf{y}, \tau | \mathbf{x}, t) / Dt^3$ be continuous everywhere else in the flow: in which case equation (2.15) would imply that $\hat{n}_j \lambda_j = 0$ on S when $p'(\mathbf{x}, t)$ is determined by the relatively simple equation

$$p'(\mathbf{x}, t) = \int_{-T}^T \int_V \frac{D_0^3 g(\mathbf{y}, \tau | \mathbf{x}, t)}{Dt^3} \tilde{\omega}_c \left(\tau - \frac{y_1}{U(\mathbf{y}_T)}, \mathbf{y}_T \right) dy d\tau \quad (2.18)$$

and (2.5) would then imply that

$$\hat{n}_i u_i(\mathbf{x}, t) = \varepsilon_{ijk} \hat{n}_i \frac{1}{c^2} \frac{\partial U}{\partial y_j} \left[\frac{\partial}{\partial y_k} \mathfrak{G} \left(\tau - \frac{y_1}{U}, \mathbf{y}_T \right) \right] \quad (2.19)$$

on the surfaces S whose generators must be parallel to the mean flow but need not extend over the entire range $-\infty < y_1 < \infty$ (i.e. they can be finite, semi-infinite or infinite in the streamwise direction). Equation (2.19) shows that $\rho v'_\perp = \hat{n}_i u_i(\mathbf{x}, t)$ will be equal to zero on S when S coincides with one or more of the constant mean velocity surfaces or, more generally, when $\mathfrak{G}(\tau - y_1/U, \mathbf{y}_T)$ is chosen so that the cross product of its gradient with the mean velocity gradient is tangent to S when $\mathbf{y}_T \in S$. The solution $p'(\mathbf{x}, t)$ to the RDT problem will then be independent of the second convected quantity $\mathfrak{G}(\tau - y_1/U, \mathbf{y}_T)$ and the acoustic field will only depend on the single convected quantity $\tilde{\omega}_c(\tau - y_1/U(\mathbf{y}_T), \mathbf{y}_T)$.

Equation (2.18) can be interpreted as a generalization of the well-known Ffowcs Williams and Hall (1970) formula (equation 6 in their paper) for the sound produced by the interaction of turbulence with an edge that is frequently used as the starting point for analyses of solid surface interactions. It is expected to provide a valid description of the flow even when the mean velocity is discontinuous across certain surfaces, which could, for example extend downstream of the solid boundaries, provided that $D_0^3 g(\mathbf{y}, \tau | \mathbf{x}, t) / Dt^3$ and $D_0^3 \gamma(\mathbf{y}, \tau | \mathbf{x}, t) / Dt^3$ remain continuous across these surfaces: in which case equation (2.15) would imply that $\hat{n}_j c^2 \lambda_j$ and $D_0 \phi / D\tau$ should be continuous there. This can be shown heuristically by considering the generic flow configuration shown schematically in figure 1 where the sub/super script + is used to denote quantities in the upper region and a minus sub/super script is used to denote quantities in the lower region. (For the sake of clarity we only show a simple flat plate configuration in the figure but the argument applies to much more general flows.)

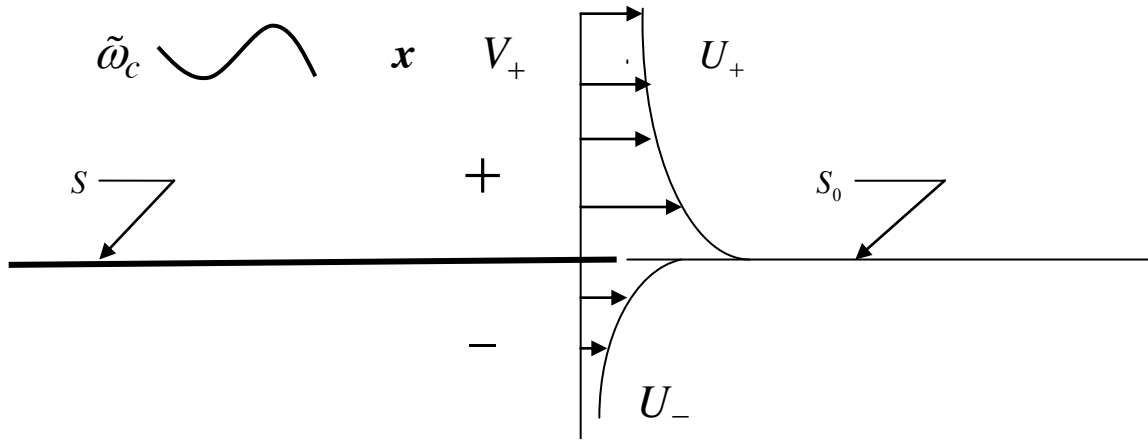


Figure 1 Wake effects

Applying equation(2.15) to the upper region and the corresponding equation derived by applying equation (2.12) and Green's theorem to the lower region shows that

$$p'(\mathbf{x}, t) = \int_{-T}^T \int_{V_+} \frac{D_0^3 g_+(\mathbf{y}, \tau | \mathbf{x}, t)}{Dt^3} \tilde{\omega}_c \left(\tau - \frac{y_1}{U(\mathbf{y}_T)}, \mathbf{y}_T \right) dy d\tau$$

$$- \int_{-T}^T \int_{S \cup S_0} \left[\frac{D_0^3 g_+(\mathbf{y}, \tau | \mathbf{x}, t)}{Dt^3} (\hat{n}_j \lambda_j^+ c^2) - \frac{D_0^3 \gamma_+(\mathbf{y}, \tau | \mathbf{x}, t)}{Dt^3} \frac{D_+^3 \phi_+}{D\tau^3} \right] dS(\mathbf{y}) d\tau \quad (2.20)$$

and

$$- \int_{-T}^T \int_{S \cup S_0} \left[\frac{D_0^3 g_-(\mathbf{y}, \tau | \mathbf{x}, t)}{Dt^3} (\hat{n}_j \lambda_j^- c^2) - \frac{D_0^3 \gamma_-(\mathbf{y}, \tau | \mathbf{x}, t)}{Dt^3} \frac{D_-^3 \phi_-}{D\tau^3} \right] dS(\mathbf{y}) d\tau = 0, \quad (2.21)$$

whenever the observation point \mathbf{x} and source function $\tilde{\omega}_c$ are confined to the upper region and the upper/lower Green's functions g_{\pm} satisfy the appropriate inhomogeneous Rayleigh equations

$$L_{\pm} g_{\pm}(\mathbf{y}, \tau | \mathbf{x}, t) = \delta(\mathbf{y} - \mathbf{x}) \delta(\tau - t) \quad (2.22)$$

together with the boundary condition (2.17) on the solid surface S . So adding equation (2.21) to (2.20) and imposing the continuity requirements

$$\gamma_+(\mathbf{y}, \tau | \mathbf{x}, t) = \gamma_-(\mathbf{y}, \tau | \mathbf{x}, t), \quad g_+(\mathbf{y}, \tau | \mathbf{x}, t) = g_-(\mathbf{y}, \tau | \mathbf{x}, t), \quad \text{for } \mathbf{y} \in S_0, \quad (2.23)$$

where the $D_{\pm}^3 \gamma_{\pm} / Dt^3$ are implicitly defined by (2.16) with $D_{\pm} / D\tau \equiv \partial / \partial \tau + U_{\pm} \partial / \partial y_1$ denoting the upper/lower convective derivatives, shows that

$$\begin{aligned}
p'(\mathbf{x}, t) = & \int_{-T}^T \int_{V_+} \frac{D_0^3 g_+(\mathbf{y}, \tau | \mathbf{x}, t)}{Dt^3} \tilde{\omega}_c \left(\tau - \frac{y_1}{U(\mathbf{y}_T)}, \mathbf{y}_T \right) dy d\tau \\
& - \int_{-T}^T \int_S \left[\frac{D_0^3 g_+(\mathbf{y}, \tau | \mathbf{x}, t)}{Dt^3} (\hat{n}_j \lambda_j^+ c^2) - \frac{D_0^3 g_-(\mathbf{y}, \tau | \mathbf{x}, t)}{Dt^3} (\hat{n}_j \lambda_j^- c^2) \right] dS(\mathbf{y}) d\tau \\
& - \int_{-T}^T \int_{S_0} \hat{n}_j \left[\frac{D_0^3 g_+(\mathbf{y}, \tau | \mathbf{x}, t)}{Dt^3} (c_+^2 \lambda_j^+ - c_-^2 \lambda_j^-) - \left(\frac{D_0^3 \gamma_+(\mathbf{y}, \tau | \mathbf{x}, t)}{Dt^3} \right) \left(\frac{D_+^3 \phi_+}{D\tau^3} - \frac{D_-^3 \phi_-}{D\tau^3} \right) \right] dS(\mathbf{y}) d\tau, \quad (2.24)
\end{aligned}$$

which, as indicated above, suggests that $\hat{n}_j c^2 \lambda_j$ and $D_0^3 \phi / D\tau^3$ will be continuous across S_0 when p' is given by equation (2.18) since g_{\pm} is required to satisfy the boundary condition (2.17) on S and $\hat{n}_j \lambda_j^{\pm}$ is still expected to be zero there: in which case equations (2.4) and (2.5) show that the physical variables will then satisfy the usual jump conditions

$$\hat{n}_i u_i^{\pm} c_{\pm}^2 = D_{\pm} (c^2 \hat{n}_i \lambda_i) / D\tau, \quad p'_+ = p'_- \text{ for } \mathbf{y}_T \in S_o. \quad (2.25)$$

The vortex sheet can, of course, support additional spatially growing instability waves that can be generated by imposing a Kutta condition at the trailing edge or suppressed by imposing a boundedness requirement on $D_0^3 g(\mathbf{y}, \tau | \mathbf{x}, t) / Dt^3$.

One difference between the present result (equation(2.18)) and the Ffowcs Williams and Hall (1970) equation is that mean flow interaction effects are now explicitly accounted for—which is an important consideration at the high Mach numbers of interest in aeronautical applications. But there are even more significant differences between these results because (unlike the present solution) the Ffowcs Williams and Hall formulation cannot be used to predict the source convection velocity, to which the calculations presented in section 6 below show great sensitivity, and does not account for trailing edge vortex shedding, which is known to have a strong effect on the directivity of the sound field. It should, however, be noted that the Rayleigh equation Green's function $g(\mathbf{y}, \tau | \mathbf{x}, t)$ is now inhomogeneous in the streamwise direction and, therefore, cannot be calculated by simply taking Fourier transforms in this direction as is usually done in classical hydrodynamic instability theory.

The transverse velocity perturbation,

$$\rho v'_{\perp}(\mathbf{x}, t) \equiv u_i(\mathbf{x}, t) \frac{\partial U}{\partial x_i} / |\nabla U|, \quad (2.26)$$

corresponding to (2.18) is given by

$$\rho v'_{\perp} = - \frac{\partial U / \partial x_i}{|\nabla U|} \int_{-T}^T \int_V g_i(\mathbf{y}, \tau | \mathbf{x}, t) \tilde{\omega}_c \left(\tau - \frac{y_1}{U(\mathbf{y}_T)}, \mathbf{y}_T \right) dy d\tau, \quad (2.27)$$

with

$$g_i(\mathbf{y}, \tau | \mathbf{x}, t) \equiv \frac{D_0}{Dt} \left(\frac{\partial}{\partial x_i} \frac{D_0}{Dt} + 2 \frac{\partial U}{\partial x_i} \frac{\partial}{\partial x_1} \right) g(\mathbf{y}, \tau | \mathbf{x}, t). \quad (2.28)$$

Inserting equation (B.12) of Goldstein, Afsar and Leib (2013) into this result, noting that the integral over the second term vanishes and that the relevant Poisson's equation Green's function is self-adjoint (i.e. $g_0(\mathbf{y}, \tau | \mathbf{x}, t) = g_0(\mathbf{x}, t | \mathbf{y}, \tau)$) shows that it reduces to (1.3) for two dimensional incompressible flows with constant mean shear when the arbitrary convected quantity $\tilde{\omega}_c(\tau - y_1 / U(\mathbf{y}_T), \mathbf{y}_T)$ is replaced by the renormalized convected quantity

$$\omega_c(\tau - y_1 / U(\mathbf{y}_T), \mathbf{y}_T) \equiv \tilde{\omega}_c(\tau - y_1 / U(\mathbf{y}_T), \mathbf{y}_T) |\nabla U| / c^2, \quad (2.29)$$

which has dimensions of vorticity (based on the rescaled velocity u_i). Equation (2.27) which, like (2.18), does not depend on the second arbitrary convected quantity $\mathfrak{G}(\tau - y_1 / U, \mathbf{y}_T)$ is, therefore, a generalization of the Orr result (1.3). The most significant difference is that the convected quantity ω_c is no longer equal to the vorticity.

Equations (2.18) and (2.27), which are the fundamental results of the paper, can be viewed as a formal solution to the complete non-homogeneous RDT problem (in the usual case where the solid surfaces are aligned with the constant velocity surfaces). They effectively reduce the RDT problem to the problem of finding the Rayleigh's equation Green's function that satisfies the appropriate boundary conditions on the bounding surfaces S . (See example problem worked out in section 6 below.)

In the absence of scattering surfaces and other external sources the unsteady motion given by equations (2.18) and (2.27) consists entirely of subsonically propagating disturbances when the general transversely sheared mean flow considered in this paper flow is purely subsonic and, therefore, cannot radiate to the far field (Goldstein, 2005 & 2009). This can easily be verified in any particular case by working out the relevant far field expansion. It is therefore appropriate to identify it with the hydrodynamic component of the motion.

3. Representation of the fundamental equations in frequency space

Taking the temporal Fourier transform of (2.18), noting that $g(\mathbf{y}, \tau | \mathbf{x}, t)$ satisfies the inhomogeneous Rayleigh equation (2.13) and, therefore, depends on τ and t only in the combination $t - \tau$ and using the convolution theorem shows that

$$\bar{p}'(\mathbf{x} : \omega) = (2\pi)^2 \int_{A_T} e^{i\omega x_1 / U(\mathbf{y}_T)} \bar{G}(\mathbf{y}_T | \mathbf{x} : \omega, \omega / U(\mathbf{y}_T)) \bar{\Omega}(\mathbf{y}_T : \omega) d\mathbf{y}_T, \quad (3.1)$$

where A_T denotes the cross sectional area corresponding to the volume V ,

$$\bar{p}'(\mathbf{x} : \omega) = \lim_{T \rightarrow \infty} \bar{p}'(\mathbf{x} : \omega, T), \quad \bar{\Omega}(\mathbf{x} : \omega) = \lim_{T \rightarrow \infty} \bar{\Omega}(\mathbf{x} : \omega, T), \quad (3.2)$$

and

$$\bar{p}'(\mathbf{x}; \omega, T) \equiv \frac{1}{2\pi} \int_{-T}^T e^{i\omega t} p'(\mathbf{x}, t) dt, \quad \bar{\Omega}(\mathbf{y}_T; \omega, T) \equiv \frac{1}{2\pi} \int_{-T}^T e^{i\omega z} \tilde{\omega}_c(z, \mathbf{y}_T) dz, \quad (3.3)$$

and

$$\bar{g}(\mathbf{y} | \mathbf{x}; \omega) \equiv \frac{1}{2\pi} \int_{-\infty}^{\infty} e^{i\omega(t-\tau)} g(\mathbf{y}, \tau | \mathbf{x}, t) d(t-\tau) \quad (3.4)$$

denote appropriate Fourier transforms. The limit

$$\bar{G}(\mathbf{y}_T | \mathbf{x}; \omega, \omega/U(\mathbf{y}_T)) \equiv \lim_{k_1 \rightarrow \omega/U(\mathbf{y}_T)} \bar{G}(\mathbf{y}_T | \mathbf{x}; \omega, k_1), \quad (3.5)$$

where

$$\bar{G}(\mathbf{y}_T | \mathbf{x}; \omega, k_1) \equiv \frac{e^{-ik_1 x_1}}{2\pi} \left[U(\mathbf{x}_T) \frac{\partial}{\partial x_1} - i\omega \right] \int_{-\infty}^{\infty} e^{ik_1 y_1} \bar{g}(\mathbf{y} | \mathbf{x}; \omega) dy_1 \quad (3.6)$$

satisfies the reduced Rayleigh equation

$$L_R \bar{G} \equiv \nabla_T \cdot \left[\frac{c^2 \nabla_T \bar{G}}{(\omega - Uk_1)^2} \right] + \left[1 - \frac{c^2 k_1^2}{(\omega - Uk_1)^2} \right] \bar{G} = \frac{1}{(2\pi)^2} \delta(\mathbf{x}_T - \mathbf{y}_T), \quad (3.7)$$

together with appropriate boundary and jump conditions, is assumed to exist--except, perhaps, at certain discrete values of \mathbf{y}_T , say $\mathbf{y}_T = \mathbf{y}_n(\omega)$, for $n=1, 2, \dots$, where \bar{G} could become singular. This could then generate potentially non-decaying modes (see, for example, Heaton and Peake, 2006) that could play an important role in the surface interaction problems, which are, of course, the primary application of the present paper. We have put $U = U(\mathbf{y}_T)$ in (3.7) and used ∇_T to denote the transverse gradient operator

$$\nabla_T \equiv \{ \partial / \partial y_2, \partial / \partial y_3 \}. \quad (3.8)$$

Proof of these assertions for an arbitrary transversely sheared mean flows is beyond the scope of the present paper, but verification for the important case of planar shear flows is given in Appendix A.

The inversion contour for the Fourier transform (3.6) should be indented around the singularities of the reduced Green's function $\bar{G}(\mathbf{y}_T | \mathbf{x}; \omega, k_1)$ in the appropriate half plane in order to satisfy the relevant causality/boundedness condition, which implies that the integration contour for \mathbf{y}_T should also be extended into the complex plane in order to insure that the relevant singularities of $\bar{G}(\mathbf{y}_T | \mathbf{x}; \omega, \omega/U(\mathbf{y}_T))$ contribute to the integral over A_T . These real axis singularities are only expected to occur at neutral instability points for the type of mean flow being considered here because the Green's function would then have a pole at the corresponding instability wave number, which must lie on the critical layer at the neutral instability point. Squire's theorem suggests that this will occur at a small number of frequencies (usually one) for any given transverse wave number (or equivalently a small number of transverse wave numbers for any given frequency) for incompressible planar mean flows.

Similar behavior is expected to occur for other mean flows including axysymmetric jets. The singularities of the reduced Green's function $\bar{G}(\mathbf{y}_T | \mathbf{x}_T : \omega, \omega/U(\mathbf{y}_T))$ are therefore, also expected to be poles – which means that their contribution to the integral over A_T would remain finite (i.e. non-zero) at large downstream distances and, therefore, dominate the flow in this region if they are included in the solution.

A similar result can be obtained for the Fourier transformed transverse velocity perturbation $\bar{v}'_{\perp}(\mathbf{x}, \omega)$ by taking the Fourier transform of (2.27) and using the inhomogeneous Rayleigh equation (3.7) to obtain

$$\rho(\mathbf{x})\bar{v}'_{\perp}(\mathbf{x}, \omega) = -(2\pi)^2 \frac{\partial U}{\partial x_i} \frac{1}{|\nabla U|} \int_{A_T} e^{i\omega x_1/U(\mathbf{y}_T)} \bar{G}_i(\mathbf{y}_T | \mathbf{x} : \omega, \omega/U(\mathbf{y}_T)) \bar{\Omega}(\mathbf{y}_T : \omega) d\mathbf{y}_T, \quad (3.9)$$

where $\bar{v}'_{\perp}(\mathbf{x}, \omega)$ is defined in terms of

$$\bar{v}'_{\perp}(\mathbf{x} : \omega; T) \equiv \frac{1}{2\pi} \int_{-T}^T e^{i\omega t} v'_{\perp}(\mathbf{x}, t) dt \quad (3.10)$$

by (3.2) and

$$\bar{G}_i(\mathbf{y}_T | \mathbf{x} : \omega, k_1) \equiv \frac{1}{[ik_1 U(\mathbf{x}_T) - i\omega]} \frac{\partial}{\partial x_i} \bar{G}(\mathbf{y}_T | \mathbf{x} : \omega, k_1). \quad (3.11)$$

Equation (3.1) is a very significant generalization of the two dimensional solution (2.38) and (2.42) of G79 since it applies to any flow in which the generators of the bounding surfaces (which can be finite or infinite in the streamwise direction) are parallel to the mean flow.

4. Relation between $\tilde{\omega}_c$ and the physical variables

The focus of this section is on the streamwise-homogeneous “gust solution” which provides an upstream boundary condition for the RDT solutions such as the one worked out in section 6 below. We can think of it as being an upstream 'input' that generates a downstream 'response' when it interacts with streamwise changes in the boundary conditions. It is desirable to relate the arbitrary convected quantities, $\tilde{\omega}_c(\tau - y_1/U, \mathbf{y}_T)$ and $\mathfrak{G}(\tau - y_1/U, \mathbf{y}_T)$, that appear in this solution to the physical (preferably measurable) flow variables in order to properly represent the upstream boundary conditions. The required relations for $\tilde{\omega}_c(\tau - y_1/U, \mathbf{y}_T)$ are worked out in this section.

The relations for $\mathfrak{G}(\tau - y_1/U, \mathbf{y}_T)$ tend to be of lesser importance in the usual case where the solid surfaces coincide with the surfaces of constant mean velocity or, more generally, when $\mathfrak{G}(\tau - y_1/U, \mathbf{y}_T)$ is chosen so that that the cross product of its gradient with the mean velocity gradient is tangent to any solid surfaces that may be present in the flow, because the scattering problem can then be formulated in terms of p' and $\rho v'_{\perp}$ and its solution will be independent of $\mathfrak{G}(\tau - y_1/U, \mathbf{y}_T)$. This quantity can, therefore, be specified after the fact when the solution is used to calculate the streamwise and circumferential velocity components u_i/ρ and $u_i/\rho - v'_{\perp}(\mathbf{x}, t)(\partial U/\partial x_i)/|\nabla U|$, for $i = 2, 3$ respectively. Goldstein et al (2013) show that $\mathfrak{G}(\tau - y_1/U, \mathbf{y}_T)$ can be expressed as a

linear combination of $\tilde{\omega}_c(\tau - y_1/U, \mathbf{y}_T)$ and the physically measurable variables. And since the results of this section relate $\tilde{\omega}_c(\tau - y_1/U, \mathbf{y}_T)$ to these variables, this effectively determines $\vartheta(\tau - y_1/U, \mathbf{y}_T)$.

The “gust solution” is most easily dealt with mathematically by dividing the Rayleigh equation Green’s function $g(\mathbf{y}, \tau | \mathbf{x}, t)$ that appears in the time dependent solutions (2.18) and (2.27) into two components, say

$$g(\mathbf{y}, \tau | \mathbf{x}, t) = g^{(0)}(\mathbf{y}, \tau | \mathbf{x}, t) + g^{(s)}(\mathbf{y}, \tau | \mathbf{x}, t), \quad (4.1)$$

where $g^{(0)}(\mathbf{y}, \tau | \mathbf{x}, t)$ is defined on all space when the bounding surfaces S are all at infinity or, more generally, satisfies (2.17) when they are not. The corresponding solution, given by (2.18) and (2.27) with $g(\mathbf{y}, \tau | \mathbf{x}, t)$ replaced by $g^{(0)}(\mathbf{y}, \tau | \mathbf{x}, t)$, represents the unsteady hydrodynamic motion on the (completely homogeneous in the y_1 -direction) doubly infinite flow that was referred to as the “gust solution” in the introduction. The remaining “scattered solution” $g^{(s)}(\mathbf{y}, \tau | \mathbf{x}, t)$ will satisfy the resulting inhomogeneous boundary and jump conditions on the streamwise discontinuous surfaces S and, therefore, be inhomogeneous in the streamwise direction.

The second “gust solution” equation given by (2.27) with $g(\mathbf{y}, \tau | \mathbf{x}, t)$ replaced by $g^{(0)}(\mathbf{y}, \tau | \mathbf{x}, t)$ can be thought of as integral equation that can be inverted to determine $\tilde{\omega}_c$ in terms of the physically measurable variable $\rho v'_\perp(\mathbf{x}, t)$. This is most easily accomplished by using the frequency representation discussed in the previous section. Corresponding to the decomposition (4.1) the reduced Rayleigh equation Green’s function $\bar{G}(\mathbf{y}_T | \mathbf{x} : \omega, k_1)$ that appears in frequency domain solutions (3.1) and (3.9) has the decomposition

$$\bar{G}(\mathbf{y}_T | \mathbf{x} : \omega, k_1) = \bar{G}^{(0)}(\mathbf{y}_T | \mathbf{x} : \omega, k_1) + \bar{G}^{(s)}(\mathbf{y}_T | \mathbf{x} : \omega, k_1), \quad (4.2)$$

where $\bar{G}^{(0)}(\mathbf{y}_T | \mathbf{x} : \omega, k_1)$ is either defined on all space when the bounding surfaces S are all at infinity or it satisfies

$$\frac{\hat{n}_j}{[\omega - k_1 U(\mathbf{y}_T)]^2} \frac{\partial}{\partial y_j} \bar{G}^{(0)}(\mathbf{y}_T | \mathbf{x} : \omega, k_1) = 0, \quad \text{for } \mathbf{y}_T \in C_T \quad (4.3)$$

(where C_T denotes the bounding curve/curves that generate the doubly infinite surface/surfaces S) when they are not.

The streamwise homogeneous Green’s functions $g^{(0)}(\mathbf{y}, \tau | \mathbf{x}, t)$ and $\bar{G}^{(0)}(\mathbf{y}_T | \mathbf{x} : \omega, k_1)$ will then depend on y_1 and x_1 only in the combination $x_1 - y_1$ and we, therefore, write

$$\bar{G}^{(0)}(\mathbf{y}_T | \mathbf{x} : \omega, k_1) = \bar{G}^{(0)}(\mathbf{y}_T | \mathbf{x}_T : \omega, k_1). \quad (4.4)$$

It would seem appropriate to require that these solutions satisfy causality (and, therefore, include contributions from the poles referred to in the previous section) if the base flow were laminar, but there

does not appear to be any evidence of spatially growing or neutral instability waves for the naturally occurring high Reynolds number turbulent base flows that are the focus of RDT. It, therefore, appears to be more appropriate to impose a weaker boundedness condition (referred to as weak causality by Dowling, Ffowcs Williams & Goldstein, 1978; see also Mani, 1976) on the applicable solution by deforming the k_1 – inversion contour for the Fourier transform (3.6) into the upper half plane. Weak causality implies that the solution satisfies the appropriate outgoing wave boundary conditions but restrictions imposed by the initial conditions are relaxed.

It follows from the second line of (3.9) that the axial Fourier Transform,

$$\rho(\mathbf{x}_T) \bar{V}_\perp^{(0)}(\mathbf{x}_T : \omega, k_1) \equiv \frac{\rho(\mathbf{x}_T)}{2\pi} \int_{-\infty}^{\infty} e^{-ik_1 x_1} \bar{v}_\perp^{(0)}(\mathbf{x} : \omega) dx_1, \quad (4.5)$$

of the density weighted “gust solution” transverse velocity $\rho(\mathbf{x}_T) \bar{v}_\perp^{(0)}(\mathbf{x}, \omega)$ spectrum is given by

$$\begin{aligned} \rho(\mathbf{x}_T) \bar{V}_\perp^{(0)}(\mathbf{x}_T : \omega, k_1) = \\ -(2\pi)^2 \frac{1}{|\nabla U|} \frac{\partial U}{\partial x_i} \int_{A_T} \delta[\omega/U(\mathbf{y}_T) - k_1] \bar{G}_i^{(0)}(\mathbf{y}_T | \mathbf{x}_T : \omega, \omega/U(\mathbf{y}_T)) \bar{\Omega}(\mathbf{y}_T : \omega) d\mathbf{y}_T, \end{aligned} \quad (4.6)$$

where $\bar{G}_i^{(0)}(\mathbf{y}_T | \mathbf{x}_T : \omega, k_1)$ is obtained by applying (3.11) to the decomposition (4.2).

Introducing any single valued coordinate transform, $\mathbf{y}_T \rightarrow \{\xi, \eta\}$, for which $U = U(\xi)$ into this result leads to the following equation

$$\begin{aligned} \rho(\mathbf{x}_T) \bar{V}_\perp^{(0)}(\mathbf{x}_T : \omega, k_1) = \\ -(2\pi)^2 \frac{1}{|\nabla U|} \frac{\partial U}{\partial x_i} \sum_n \frac{1}{|\kappa'_n|} \int_{C_n} \bar{G}_i^{(0)}(\mathbf{y}_T(\xi_n, \eta) | \mathbf{x}_T : \omega, k_1) \bar{\Omega}(\mathbf{y}_T(\xi_n, \eta) : \omega) J(\xi_n, \eta) d\eta, \end{aligned} \quad (4.7)$$

where $J(\xi, \eta) = \partial(y_2, y_3) / \partial(\xi, \eta)$ denotes the Jacobian, \int_{C_n} denotes the integral over curves of constant $\xi_n(k_1)$, with $\xi_n(k_1)$ being the nth root of

$$\kappa(\xi_n) = k_1, \quad (4.8)$$

where

$$\kappa(\xi) \equiv \omega/U(\xi) \text{ and } \kappa'_n \equiv d\kappa/d\xi|_{\xi=\xi_n}, \quad (4.9)$$

and the sum is over the N roots of (4.9). By preselecting a set of N discrete points, say

$$\mathbf{x}_T = \{\mathbf{x}_T^{(1)}, \mathbf{x}_T^{(2)}, \mathbf{x}_T^{(3)}, \dots, \mathbf{x}_T^{(N)}\},$$

equation (4.7) can be used to obtain a coupled set of integral equations that can, in principle, be solved numerically to determine the unknown convected quantity

$\bar{\Omega}(\mathbf{y}_T(\xi_n, \eta) : \omega)$ in terms of the Fourier transformed physical variable $\rho(\mathbf{x}_T) \bar{V}_\perp^{(0)}(\mathbf{x}_T : \omega, k_1)$

evaluated at these points. The kernel will also have to be computed numerically since

$\bar{G}^{(0)}(\mathbf{y}_T(\xi, \eta) | \mathbf{x}_T : \omega, k_1)$ and, therefore, $\bar{G}_i^{(0)}(\mathbf{y}_T(\xi, \eta) | \mathbf{x}_T : \omega, k_1)$ will satisfy a partial differential equation (obtained from (3.7) under the change of variable $\mathbf{y}_T \rightarrow (\xi, \eta)$) whose coefficients depend on both ξ and η .

Analytical results can, however, be obtained in the important special cases where (ξ, η) are polar or rectangular coordinates since the coefficient of the differential equation for $\bar{G}^{(0)}(\mathbf{y}_T(\xi, \eta) | \mathbf{x}_T : \omega, k_1)$ will then be independent of η . The transformed Green's function $\bar{G}^{(0)}(\mathbf{y}_T(\xi, \eta) | \mathbf{x}_T : \omega, k_1)$ $\partial(\hat{\xi}, \hat{\eta}) / \partial(x_2, x_3)$, where $(\hat{\xi}, \hat{\eta})$ denote the corresponding change in variable $\mathbf{x}_T \rightarrow (\hat{\xi}, \hat{\eta})$ such that $U(\mathbf{x}_T) = U(\hat{\xi})$, will then depend on η and $\hat{\eta}$ only in the combination $\eta - \hat{\eta}$ when each of the bounding surfaces extends over a complete $\xi = \text{constant}$ curve. (It is again important to note that these requirements only apply to the "gust solution" and not to the downstream "scattered solution", which can be completely unrestricted.)

For definiteness, we only consider the case where ξ, η denotes the rectangular coordinate system $\xi = y_2, \eta = y_3$ for which the Jacobian is unity (i.e., a two dimensional mean flow). It then follows from the convolution theorem that

$$\begin{aligned} \hat{V}_\perp^{(0)}(x_2, y_2, \omega, k_3) &\equiv \frac{1}{2\pi} [\text{sgn } U'(x_2)] \int_{-\infty}^{\infty} e^{-ix_3 k_3} \rho(\mathbf{x}_T) \bar{V}_\perp^{(0)}(\mathbf{x}_T : \omega, \omega / U(y_2)) dx_3 \\ &= -(2\pi)^3 \sum_n \frac{1}{|\kappa'_n|} \hat{G}_2^{(0)}(y_2^{(n)} | x_2 : \omega, \omega / U(y_2), k_3) \hat{\Omega}(y_2^{(n)} : \omega, k_3), \end{aligned} \quad (4.10)$$

where the κ'_n 's are given by (4.9), $y_2^{(n)}$ is the n th root of

$$U(y_2^{(n)}) = U(y_2), \text{ for } n = 1, 2, \dots, N, \quad (4.11)$$

$$\hat{\Omega}(y_2 : \omega, k_3) \equiv \frac{1}{2\pi} \int_{-\infty}^{\infty} e^{-iy_3 k_3} \bar{\Omega}(\mathbf{y}_T : \omega) dy_3, \quad (4.12)$$

$$\hat{G}_i^{(0)}(y_2^{(n)} | x_2 : \omega, k_1, k_3) \equiv \frac{1}{2\pi} \int_{-\infty}^{\infty} e^{i(y_3 - x_3) k_3} \bar{G}_i^{(0)}(y_2^{(n)}, y_3 | x_2, x_3, 0 : \omega, k_1) d(y_3 - x_3), i = 2, 3 \quad (4.13)$$

is just the spanwise Fourier transform of $\bar{G}_i^{(0)}(\mathbf{y}_T | \mathbf{x}_T : \omega, k_1)$ (since $\hat{\xi} = x_2$ and $\hat{\eta} = x_3$ in this case) and y_2 can be restricted to lie in an appropriate range.

Then since $\hat{\Omega}(y_2^{(n)}(y_2) : \omega, k_3)$ only depends on y_2 with y_2 in this range while $\hat{V}_\perp^{(0)}(x_2, y_2, \omega, k_3)$ and $\hat{G}_2^{(0)}(y_2^{(n)} | x_2 : \omega, \omega / U(y_2), k_3)$ depend on y_2 and x_2 , equation (4.10) shows that the $\hat{V}_\perp^{(0)}(x_2, y_2, \omega, k_3)$ can only be specified at N discrete points, say $x_2^{(1)}, x_2^{(2)}, \dots, x_2^{(N)}$. This leads to a set

of N linear algebraic equations in the N unknown $\hat{\Omega}(y_2^{(n)}(y_2) : \omega, k_3), n=1, 2, \dots, N$, or equivalently a matrix equation with matrix elements $(2\pi)^3 \hat{G}_2^{(0)}(y_2^{(n)} | x_2 : \omega, \omega/U(y_2), k_3) / |\kappa'_n|$. The latter can be inverted to obtain a unique solution vector $\left\{ \hat{\Omega}(y_2^{(1)}(y_2) : \omega, k_3), \hat{\Omega}(y_2^{(2)}(y_2) : \omega, k_3), \dots, \hat{\Omega}(y_2^{(N)}(y_2) : \omega, k_3) \right\}$, when the determinant of the matrix is non-zero. The $\hat{V}_\perp^{(0)}(x_2, y_2, \omega, k_3)$ are determined at all other $x_2 \neq x_2^{(1)}, x_2^{(2)}, \dots, x_2^{(N)}$ by inserting this result into equation(4.10). The matrix equation can also be solved when its determinant is equal to zero if the source vector $\left\{ \hat{V}_\perp^{(0)}(x_2^{(1)}, y_2, \omega, k_3), \hat{V}_\perp^{(0)}(x_2^{(2)}, y_2, \omega, k_3), \dots, \hat{V}_\perp^{(0)}(x_2^{(N)}, y_2, \omega, k_3) \right\}$ is required to satisfy certain solvability conditions (i.e., that it is orthogonal to the eigenvectors of the transposed matrix). This means that the number N' of points at which the $\hat{V}_\perp^{(0)}(x_2, y_2, \omega, k_3)$ can be specified will be less than N and there will, therefore, be certain arbitrariness in the choice of $\hat{\Omega}(y_2^{(n)} : \omega, k_3)$ since the solution to the matrix equation will be non-unique.

In planar shear flow with monotonic velocity profile equation (4.11) will have only one root and therefore the sum in equation(4.10) will contain a single term. This equation can then be inverted to obtain

$$\hat{\Omega}(y_2 : \omega, k_3) = \frac{-|\kappa'_n| \hat{V}_\perp^{(0)}(x_2^{(1)}, y_2, \omega, k_3)}{(2\pi)^4 \hat{G}_2^{(0)}(y_2 | x_2^{(1)} : \omega, \omega/U(y_2), k_3)}. \quad (4.14)$$

Equation (4.11) will have two roots for jet like flows where the mean velocity profile has a single maximum: in which case there will be two terms in the sum over n in equation(4.10) at any given value of x_2 . Since it is appropriate to require that the source points be symmetrically placed when the velocity profile is symmetric about the single point $y_2 = y_d$ we can write the matrix equation for this case as

$$\begin{bmatrix} \hat{V}_\perp^{(0)}(x_2^{(1)}, y_2, \omega, k_3) \\ \hat{V}_\perp^{(0)}(x_2^{(2)}, y_2, \omega, k_3) \end{bmatrix} = -(2\pi)^3 \frac{U^2(y_2)}{\omega |U'(y_2)|} \times \begin{bmatrix} \hat{G}_2^{(0)}(y_2 | x_2^{(1)} : \omega, \omega/U(y_2), k_3) \hat{G}_2^{(0)}(2y_d - y_2 | x_2^{(1)} : \omega, \omega/U(y_2), k_3) \\ \hat{G}_2^{(0)}(y_2 | x_2^{(2)} : \omega, \omega/U(y_2), k_3) \hat{G}_2^{(0)}(2y_d - y_2 | x_2^{(2)} : \omega, \omega/U(y_2), k_3) \end{bmatrix} \begin{bmatrix} \hat{\Omega}(y_2 : \omega, k_3) \\ \hat{\Omega}(2y_d - y_2 : \omega, k_3) \end{bmatrix}, \quad (4.15)$$

for $y_2 \leq y_d$. The Greens function $\hat{G}_2^{(0)}(y_2 | x_2^{(1)} : \omega, \omega/U(y_2), k_3)$, for velocity profiles of this type, where the inverse mapping $U(y_2) \rightarrow y_2$ is double valued, will have a critical layer singularity at the symmetrically located point $U(y_2^{(2)}) = U(y_2)$ in addition to fundamental singularity at the source

point y_2 discussed in Appendix A. This causes some difficulty because (as shown in Appendix C) the Rayleigh equations usually have to be integrated through this point in order to satisfy the requisite boundary conditions. But since there is some flexibility in the choice of Green's function, we can eliminate these difficulties by allowing the Greens function to be complex and avoiding the second critical layer singularity by supposing that $\omega/k_1 = U(y_2)$ has a small imaginary part that is set to zero after the Green's function has been calculated (as is usually done in applying the Briggs (1964)-Bers (1975) procedure and as is done implicitly in working out the Wiener Hopf factorization in section 6.3 below). This procedure is made more explicit in the specific example worked out in section 6.3 (see comments below equation(6.36)).

For more general mean flows and bounding surface geometries $\bar{\Omega}(y_T : \omega)$ has to be determined by solving the integral equation (4.7) in the single independent variable η or perhaps a finite set of such equations for non-monotonic velocity profiles.

The resulting solutions $\hat{\Omega}(y_2^{(n)}(y_2) : \omega, k_3)$, for $n=1,2$ can then be inserted into(3.3) and (4.12) and the Fourier transforms can be inverted to calculate the unknown source functions $\tilde{\omega}_c(t - x_1/U(y_T), y_T)$ in terms of Fourier transforms of the "gust solution" transverse velocities at certain preselected points, which can be interpreted as the pressures/transverse velocities that would exist at those points in the absence of the scattering edges. These latter quantities therefore, provide appropriate upstream initial/boundary conditions for the RDT turbulence/solid surface interaction problem. But since the problem is linear, it follows from (3.9),(4.2)and (4.4) that the complete solution to any problem where the surface extends continuously from $-\infty < x_3 < \infty$, say for the Fourier transformed transverse velocity fluctuation $\hat{v}'_{\perp}(x_1, x_2; k_3, \omega)$, must be of the form

$$\hat{v}'_{\perp}(x_1, x_2; \omega, k_3) = \int_{l_T} \mathcal{R}(y_2 | x_1, x_2; \omega, k_3) \hat{\Omega}(y_2 : \omega, k_3) dy_2, \quad (4.16)$$

knowledge of $\hat{\Omega}(y_2 : \omega, k_3)$ is all that is actually needed. A similar formula would, of course, also hold for Fourier transformed pressure fluctuation $\hat{p}'(x_1, x_2; \hat{k}, \omega)$ (see, for example, equation (6.1)below).

5. Relation between the $\tilde{\omega}_c$ spectra and measurable turbulence correlations

But only statistical quantities, such as

$$v'_{\perp}(\mathbf{x}, t) v'_{\perp}(\tilde{\mathbf{x}}, t + \tau) \equiv \lim_{T \rightarrow \infty} \frac{1}{2T} \int_{-T}^T v'_{\perp}(\mathbf{x}, t) v'_{\perp}(\tilde{\mathbf{x}}, t + \tau) dt \quad (5.1)$$

are of interest for the time stationary turbulent flows that are the main focus of RDT. For simplicity, we only consider mean flows that are uniform in the x_3 - direction and suppose that the turbulence is homogeneous in the spanwise direction. Then the space-time average

$$\left\langle v'_{\perp}(\mathbf{x}, t) v'_{\perp}(x_1, \tilde{x}_2, x_3 + \eta_3, t + \tau) \right\rangle \equiv \lim_{T \rightarrow \infty} \frac{1}{2T} \int_{-T}^T \int_{-\infty}^{\infty} v'_{\perp}(\mathbf{x}, t) v'_{\perp}(x_1, \tilde{x}_2, x_3 + \eta_3, t + \tau) dt dx_3 \quad (5.2)$$

will exist and be independent of t , x_3 and, it follows from the convolution theorem that

$$\begin{aligned} \frac{1}{(2\pi)^2} \int_{-\infty}^{\infty} \int_{-\infty}^{\infty} e^{i(\omega\tau - k_3\eta_3)} \left\langle v'_{\perp}(\mathbf{x}, t) v'_{\perp}(x_1, \tilde{x}_2, x_3 + \eta_3, t + \tau) \right\rangle d\tau d\eta_3 \\ = (2\pi)^2 \lim_{T \rightarrow \infty} \frac{\hat{v}'_{\perp}(x_1, x_2; \omega, k_3; T) \hat{v}'_{\perp}[(x_1, \tilde{x}_2; \omega, k_3; T)]^*}{2T}, \end{aligned} \quad (5.3)$$

where the asterisk denotes the complex conjugate and the notation for the Fourier transform, $\hat{v}'_{\perp}(x_1, x_2; \omega, k_3; T)$, is the same as that used in (3.2) and (3.3). The spectrum (5.3) of the RDT solution (4.16) is, therefore, given by

$$\begin{aligned} \frac{1}{(2\pi)^2} \int_{-\infty}^{\infty} \int_{-\infty}^{\infty} e^{i(\omega\tau - k_3\eta_3)} \left\langle v'_{\perp}(\mathbf{x}, t) v'_{\perp}(x_1, \tilde{x}_2, x_3 + \eta_3, t + \tau) \right\rangle d\tau d\eta_3 = \\ \int_{L_T} \int_{L_T} \mathcal{R}(y_2 | x_1, x_2; \omega, k_3) \mathcal{R}^*(y_2 | x_1, \tilde{x}_2; \omega, k_3) S(y_2, \tilde{y}_2; \omega, k_3) dy_2 d\tilde{y}_2, \end{aligned} \quad (5.4)$$

where L_T denotes the range of the y_2 -integration. The spectrum

$$\begin{aligned} S(y_2, \tilde{y}_2; k_3, \omega) \equiv (2\pi)^2 \lim_{T \rightarrow \infty} \frac{\hat{\Omega}(y_2; \omega, k_3; T) \hat{\Omega}^*(\tilde{y}_2; \omega, k_3; T)}{2T} \\ = \frac{1}{2\pi} \int_{-\infty}^{\infty} \int_{-\infty}^{\infty} e^{i(\omega\tau - k_3\eta_3)} \left\langle \tilde{\omega}_c(t, y_T) \tilde{\omega}_c(t + \tau, \tilde{y}_2, y_3 + \eta_3) \right\rangle d\tau d\eta_3, \end{aligned} \quad (5.5)$$

of the convected quantity $\tilde{\omega}_c$ (or source function) is independent of the streamwise coordinate y_1 (even though the RDT solution spectrum is x_1 -dependent). Then since $\hat{\Omega}(y_2; \omega, k_3) = \hat{\Omega}(y_2^{(n)}; \omega, k_3)$ for y_2 in the appropriate range as n varies from 1 to N , the solution to the matrix equation obtained from (4.10) can be inserted into this result to relate S to the experimentally measurable transverse velocity spectrum

$$F_{\perp}(x_2, \tilde{x}_2 | y_2, \tilde{y}_2, \omega, k_3) \equiv \lim_{T \rightarrow \infty} \frac{1}{2T} \hat{V}_{\perp}^{(0)}(x_2, y_2, \omega, k_3; T) \left[\hat{V}_{\perp}^{(0)}(\tilde{x}_2, \tilde{y}_2, \omega, k_3; T) \right]^*, \quad (5.6)$$

evaluated at the N^2 discrete points $x_2^{(1)}, x_2^{(2)}, \dots, x_2^{(N)}, \tilde{x}_2^{(1)}, \tilde{x}_2^{(2)}, \dots, \tilde{x}_2^{(N)}$ when the base flow is two dimensional.

Equation (4.14) shows that this result, which only involves $F_{\perp}(x_2|y_2, \tilde{y}_2, \omega, k_3)$ $= F_{\perp}(x_2, x_2|y_2, \tilde{y}_2, \omega, k_3)$ evaluated at the single point $x_2^{(1)}$, can be written down explicitly as

$$S(y_2, \tilde{y}_2 : k_3, \omega) = \frac{\omega^2 F_{\perp}(x_2^{(1)}|y_2, \tilde{y}_2, \omega, k_3) |U'(y_2)U'(\tilde{y}_2)|}{(2\pi)^6 \hat{G}_2^{(0)}(y_2|x_2^{(1)} : \omega, \omega/U(y_2), k_3) \left[\hat{G}_2^{(0)}(\tilde{y}_2|x_2^{(1)} : \omega, \omega/U(\tilde{y}_2), k_3) \right]^* [U(y_2)U(\tilde{y}_2)]^2} \quad (5.7)$$

when mean velocity profile is monotonic. All the factors in this equation except $F_{\perp}(x_2|y_2, \tilde{y}_2, \omega, k_3)$, which is independent of the streamwise coordinate y_1 , can be calculated once the mean flow is specified. But this function *is related to the y_1 -independent--experimentally determinable--quantity*

$$f_{\perp}(x_2, \tilde{x}_2|k_1, \tilde{k}_1, \eta_3, \tau) \equiv \frac{1}{(2\pi)^2} \int_{-\infty}^{\infty} \int_{-\infty}^{\infty} e^{-i(x_1 k_1 - \tilde{x}_1 \tilde{k}_1)} \langle \rho v_{\perp}^{(0)}(\mathbf{x}, t) \rho v_{\perp}'^{(0)}(\tilde{x}_1, \tilde{x}_2, x_3 + \eta_3, t + \tau) \rangle dx_1 d\tilde{x}_1, \quad (5.8)$$

with

$$\langle \rho v_{\perp}^{(0)}(\mathbf{x}, t) \rho v_{\perp}'^{(0)}(\tilde{x}_1, \tilde{x}_2, x_3 + \eta_3, t + \tau) \rangle \equiv \lim_{T \rightarrow \infty} \frac{1}{2T} \int_{-T}^T \int_{-\infty}^{\infty} \rho v_{\perp}^{(0)}(\mathbf{x}, t) \rho v_{\perp}'^{(0)}(\tilde{x}_1, \tilde{x}_2, x_3 + \eta_3, t + \tau) dt dx_3, \quad (5.9)$$

since applying the convolution theorem to (5.6) and using the definitions (4.5) and (4.10) shows that

$$F_{\perp}(x_2, \tilde{x}_2|y_2, \tilde{y}_2, \omega, k_3) = \frac{1}{(2\pi)^2} \int_{-\infty}^{\infty} \int_{-\infty}^{\infty} e^{-i(\omega \tau - k_3 \eta_3)} f_{\perp}(x_2, \tilde{x}_2|\omega/U(y_2), \omega/U(\tilde{y}_2), \eta_3, \tau) d\eta_3 d\tau. \quad (5.10)$$

This means that the streamwise independent transverse velocity *correlation* (5.8) *will provide a suitable y_1 -independent upstream boundary condition for the RDT problem in this case*—provided, of course, that the integrals exist. This issue will be discussed in more detail when a specific model is introduced for $\langle \rho v_{\perp}^{(0)}(\mathbf{x}, t) \rho v_{\perp}'^{(0)}(\tilde{x}_1, \tilde{x}_2, x_3 + \eta_3, t + \tau) \rangle$ in sections 6.4 and 6.5. A similar result can, of course, be written down in terms of the pressure correlation.

6. Application to the jet -plate interaction problem

The purpose of this section is to demonstrate how the generalized RDT formulation developed in this paper can be used to solve surface interaction problems of practical interest. To this end, we apply the theory to the problem of a two-dimensional jet interacting with the downstream edge of the semi-infinite plate. A schematic of the problem is shown in figure 2. This relatively simple geometry can be used to represent the experimental configuration of a subsonic jet emanating from a large-aspect-ratio rectangular nozzle in the vicinity of a flat plate recently considered at NASA Glenn (Zaman, Bridges & Brown, 2013; Bridges and Brown 2013). A Computer -Aided design (CAD) drawing of the experimental set up is shown in figure 3.

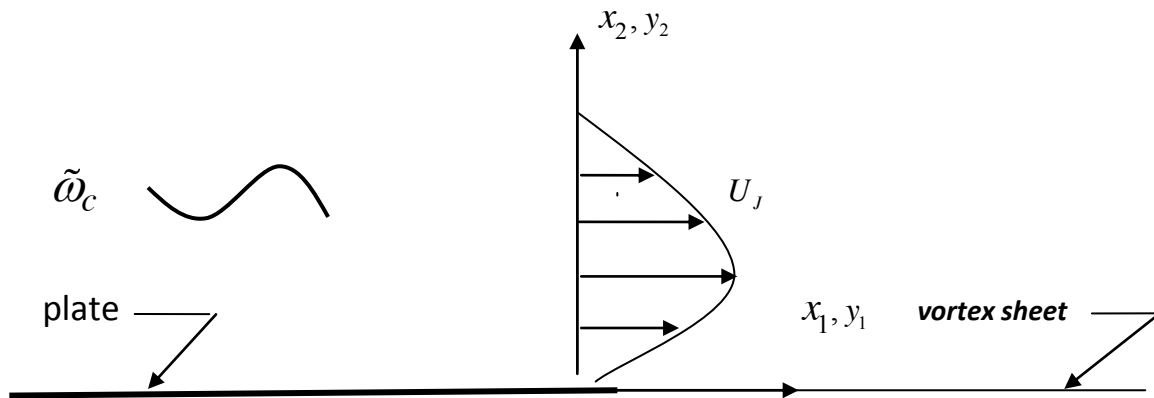


Figure 2 Computational model of the Jet/surface interaction problem

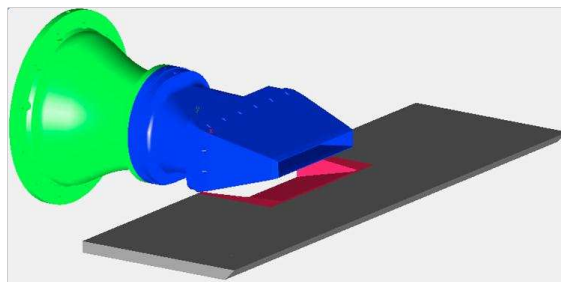


Figure 3 Experimental Configuration for jet surface interaction. Figure courtesy Dr. James E. Bridges, NASA Glenn.

The problem illustrated in figure 2 is formulated in the next sub-section and the fundamental equation (2.18) is used to obtain the solution. The result is then utilized to obtain a formula for the acoustic spectrum of the noise generated by the interaction of the jet with the trailing edge in terms of the spectrum of the arbitrary convected quantity $\tilde{\omega}_c$. This quantity cannot, however, be measured experimentally and the results developed in section 5 of this paper are, therefore, used to relate it to the transverse velocity spectrum, which we then represent by the experimentally based model (6.45) below. The result is used to obtain predictions of the noise generated by the trailing edge interaction which are then compared with the NASA Glenn data in section 6.5.

6.1 Formulation

We suppose that the vortical disturbance $\tilde{\omega}_c$ is confined to the jet and that the mean flow is everywhere subsonic. Then, since the base flow is two dimensional, it follows that $\bar{G}(\mathbf{y}_T | \mathbf{x} : \omega, k_1)$ will depend on x_3, y_3 only in the combination $x_3 - y_3$. Taking the x_3 -Fourier transform of equation(3.1) yields

$$\hat{p}'(x_1, x_2 : \omega, k_3) \equiv \frac{1}{2\pi} \int_{-\infty}^{\infty} e^{-ik_3 x_3} \bar{p}'(\mathbf{x} : \omega) dx_3 =$$

$$= (2\pi)^3 \int_0^\infty e^{i\omega x_1/U(y_T)} \hat{G}(y_2 | x_1, x_2 : \omega, \omega/U(y_2), k_3) \hat{\Omega}(y_2 : \omega, k_3) dy_2, \quad (6.1)$$

where

$$\hat{G}(y_2 | x_1, x_2 : \omega, k_1, k_3) = \hat{G}^{(0)}(y_2 | x_2 : \omega, k_1, k_3) + \hat{G}^{(s)}(y_2 | x_1, x_2 : \omega, k_1, k_3), \quad (6.2)$$

with $\hat{\Omega}(y_2 : \omega, k_3)$ given by (4.12). Equation (3.7) shows that the “gust solution”

$$\hat{G}^{(0)}(y_2 | x_2 : \omega, k_1, k_3) \equiv \frac{1}{2\pi} \int_{-\infty}^\infty e^{i(y_3-x_3)k_3} \bar{G}^{(0)}(y_T | x_T : \omega, k_1) d(y_3 - x_3) \quad (6.3)$$

satisfies the reduced inhomogeneous Rayleigh equation (A.3) with $U(y_2) = U_j(y_2)$, for $y_2 \geq 0$,

$U(y_2) = 0$ for $y_2 \leq 0$ and

$$\hat{G}_{>/<}(y_2 | x_1, x_2 : \omega, k_1, k_3) \equiv e^{ik_1 x_1} \hat{G}^{(s)}(y_2 | x_1, x_2 : \omega, k_1, k_3) \quad (6.4)$$

$$= \frac{1}{2\pi} e^{ik_1 x_1} \int_{-\infty}^\infty e^{ik_3(y_3-x_3)} \bar{G}^{(s)}(y_T | x : \omega, k_1) dy_3, \quad \text{for } y_2 > / < 0$$

are specific homogeneous solutions of this equation that have outgoing wave behavior at $y_2 = \pm\infty$ respectively. The gust component $\hat{G}^{(0)}(y_2 | x_2 : \omega, k_1, k_3)$ can be identified with the inhomogeneous solution (A.4) of (A.3) that satisfies the homogeneous boundary condition

$$\partial \hat{G}_0 / \partial y_2 = 0, \quad \text{for } y_2 = 0, -\infty < y_1 < \infty \quad (6.5)$$

with $\hat{P}_\pm(x_2)$ interpreted as the homogeneous solution that exhibits outgoing wave behavior at $x_2 = \pm\infty$ and $\hat{P}_\mp(y_2)$ interpreted as the second linearly independent solution that satisfies the homogeneous boundary condition (6.5) when the source coordinate y_2 is positive/negative.

Applying the jump conditions (2.23) and using (2.16), (2.17), (3.4), (3.6), (6.4), (6.5) now leads to the following Wiener Hopf problem for $\hat{G}_{>/<}$

$$\int_{-\infty}^\infty e^{-ik_1 y_1} (k_1 U_s / \omega - 1)^{-2} \hat{G}'_>(0 | x_1, x_2 : \omega, k_1, k_3) dk_1 =$$

$$\frac{1}{(2\pi)^2} e^{ik_1 x_1} \int_{-\infty}^\infty \int_{-\infty}^\infty e^{i\omega(t-\tau)} e^{ik_3(y_3-x_3)} \gamma(y, \tau | x, t) d(t-\tau) dy_3 = 0, \quad -\infty < y_1 < 0, \quad (6.6)$$

$$\begin{aligned} & \int_{-\infty}^{\infty} e^{-ik_1 y_1} (k_1 U_s / \omega - 1)^{-2} \hat{G}'_{>}(0 | x_1, x_2 : \omega, k_1, k_3) dk_1 \\ &= \int_{-\infty}^{\infty} e^{-ik_1 y_1} \hat{G}'_{<}(0 | x_1, x_2 : \omega, k_1, k_3) dk_1, \quad -\infty < y_1 < \infty, \end{aligned} \quad (6.7)$$

and

$$\begin{aligned} & \text{sgn}(x_2) \int_{-\infty}^{\infty} e^{ik_1(x_1 - y_1)} \hat{G}^{(0)}(0 | x_2 : \omega, k_1, k_3) dk_1 + \int_{-\infty}^{\infty} e^{-ik_1 y_1} \hat{G}'_{>}(0 | x_1, x_2 : \omega, k_1, k_3) dk_1 \\ &= \int_{-\infty}^{\infty} e^{-ik_1 y_1} \hat{G}'_{<}(0 | x_1, x_2 : \omega, k_1, k_3) dk_1, \quad 0 < y_1 < \infty, \end{aligned} \quad (6.8)$$

where

$$U_s \equiv U_J(0), \quad c_s \equiv c(0), \quad (6.9)$$

$$\hat{G}'_{> <}(0 | x_1, x_2 : \omega, k_1, k_3) \equiv \partial \hat{G}_{> <}(y_2 | x_1, x_2 : \omega, k_1, k_3) / \partial y_2 \Big|_{y_2=0}, \quad \hat{P}'_{> <}(0 : \omega, k_1, k_3) \equiv \partial \hat{P}_{> <}(y_2 : \omega, k_1, k_3) / \partial y_2 \Big|_{y_2=0}$$

and we assume, subject to subsequent verification, that $\hat{G}_{> <}(y_2 | x_1, x_2 : \omega, k_1, k_3)$ does not become exponentially large as $k_1 \rightarrow \infty$, $0 \leq \arg k_1 < 2\pi$. Since outgoing wave solutions to (A.3) corresponding to any fixed value of ω, k_1, k_3 can only differ from one another by a multiplicative constant, the specific solutions $\hat{G}_{> <}(y_2 | x_1, x_2 : \omega, k_1, k_3)$ are related to *arbitrary* homogeneous solutions $\hat{P}_{> <}(y_2 : \omega, k_1, k_3)$ that have this behavior by

$$\frac{\hat{G}_{> <}(y_2 | x_1, x_2 : \omega, k_1, k_3)}{\hat{G}'_{> <}(0 | x_1, x_2 : \omega, k_1, k_3)} = \frac{\hat{P}_{> <}(y_2 : \omega, k_1, k_3)}{\hat{P}'_{> <}(0 : \omega, k_1, k_3)}. \quad (6.10)$$

The Wiener Hopf problem(6.6)-(6.8) can easily be solved by standard methods (Nobel, 1988; Crighton and Leppington, 1970; Jaworski and Peake, 2013). Details are given in Appendix B for completeness sake. The results show that the Fourier transformed pressure $\hat{p}'(x_1, x_2 : \omega, k_3)$ is given by

$$\begin{aligned} \hat{p}'(x_1, x_2 : \omega, k_3) &= (2\pi)^3 H(x_2) \int_0^{\infty} e^{i\omega x_1 / U(y_2)} \hat{G}^{(0)}(y_2 | x_2 : \omega, \omega / U(y_2), k_3) \hat{\Omega}(y_2 : \omega, k_3) dy_2 \\ &+ (2\pi)^3 \int_0^{\infty} \frac{(U_s / U(y_2) - 1)^2 \hat{P}_{>}(y_2 : \omega, \omega / U(y_2), k_3)}{\hat{P}'_{>}(0 : \omega, \omega / U(y_2), k_3)} R(y_2 | x_1, x_2 : k_3; \omega) \hat{\Omega}(y_2 : \omega, k_3) dy_2, \end{aligned} \quad (6.11)$$

where $H(x_2)$ denotes the Heaviside function

$$R(y_2 | x_1, x_2 : k_3; \omega) \equiv \frac{1}{2\pi i} \int_{-\infty}^{\infty} e^{ik_1 x_1} \frac{\kappa_-(k_1, k_3) \text{sgn}(x_2) \hat{G}^{(0)}(0 | x_2 : k_1, k_3, \omega)}{\kappa_+(\omega / U(y_2), k_3) [\omega / U(y_2) - k_1]} dk_1, \quad (6.12)$$

and $\kappa_{\pm}(k_1, k_3)$ denote bounded analytic functions in the upper/lower half planes that satisfy the factorization condition

$$\kappa_+(k_1, k_3)/\kappa_-(k_1, k_3) = \Gamma_0(\omega, k_1, k_3) = (k_1 U_s / \omega - 1)^2 \frac{\hat{P}_>(0 : \omega, k_1, k_3)}{\hat{P}'_>(0 : \omega, k_1, k_3)} - \frac{\hat{P}_<(0 : \omega, k_1, k_3)}{\hat{P}'_<(0 : \omega, k_1, k_3)} \quad (6.13)$$

on the real k_1 -axis with the k_1 -integration contour in (6.12) being deformed to pass below the pole at $\omega/U(y_2) = k_1$. We can, however, interpret this integral as a Cauchy principle value when evaluating the far field behavior of (6.11), since the contribution from that pole produces a term that behaves like $\exp[i\omega x_1 / U(y_2)]$, which combines with the first term in (6.11) to produce a non-radiating disturbance at subsonic speeds.

It now follows from the convolution theorem that

$$\overline{p^s}(\mathbf{x}; \omega) = (2\pi)^2 \int_{-\infty}^{\infty} \int_0^{\infty} \mathcal{R}(y_2 | x_1, x_2, x_3 - y_3 : \omega) \bar{\Omega}(y_T : \omega) dy_2 dy_3, \quad (6.14)$$

where

$$\begin{aligned} \mathcal{R}(y_2 | \mathbf{x} : \omega) &= \int_{-\infty}^{\infty} e^{ik_3 x_3} R(y_2 | x_1, x_2 : k_3; \omega) (U_s / U(y_2) - 1)^2 \frac{\hat{P}_>(y_2 : \omega, \omega / U(y_2), k_3)}{\hat{P}'_>(0 : \omega, \omega / U(y_2), k_3)} dk_3 \\ &= \frac{1}{2\pi i} \int_{-\infty}^{\infty} \int_{-\infty}^{\infty} e^{i(k_1 x_1 + k_3 x_3)} \frac{\kappa_-(k_1, k_3) \operatorname{sgn}(x_2) \hat{G}^{(0)}(0 | x_2 : k_1, k_3, \omega)}{\kappa_+(\omega / U(y_2), k_3) [\omega / U(y_2) - k_1]} \\ &\quad \times \frac{(U_s / U(y_2) - 1)^2 \hat{P}_>(y_2 : \omega, \omega / U(y_2), k_3)}{\hat{P}'_>(0 : \omega, \omega / U(y_2), k_3)} dk_3 dk_1 \end{aligned} \quad (6.15)$$

The (y_2 -independent) invariant Δ given by (A.5) can be evaluated at $y_2 = 0$ and the boundary condition (6.5) can be used in (A.5) to obtain

$$\Delta(\omega, k_1, k_3) \equiv \pm \frac{(2\pi)^3 c_s^2 \hat{P}_{\mp}(0) \hat{P}'_{>/<}(0)}{[\omega - H(x_2) U_s k_1]^2} \quad \text{for } x_2 > / < 0, \quad (6.16)$$

which can be inserted into (A.4) to show that $\hat{G}^{(0)}(0 | x_2 : k_1, k_3, \omega)$ can be written as

$$\operatorname{sgn}(x_2) \hat{G}^{(0)}(0 | x_2 : \omega, k_1, k_3) = \frac{\omega^2 [\omega - H(x_2) U_s k_1]^2 \hat{P}_{>/<}(x_2 : \omega, k_1, k_3)}{(2\pi)^3 c_s^2 \hat{P}'_{>/<}(0 : \omega, k_1, k_3)} \quad \text{for } x_2 > / < 0 \quad (6.17)$$

where U_s is defined by (6.9).

For aeroacoustic applications the interest is usually in the far field acoustic spectrum.

6.2 Far field behavior and the acoustic spectrum

Since the arbitrary outgoing wave Rayleigh's equation solutions $\hat{P}_{>/<}(x_2; k_1, k_3, \omega)$ behave like

$$\hat{P}_{>/<}(x_2; k_1, k_3, \omega) \rightarrow A_{>/<}(k_1, k_3, \omega) \exp - \sqrt{k_1^2 + k_3^2 - k_\infty^2} |x_2|, \text{ as } |x_2| \rightarrow \infty \quad (6.18)$$

where $k_\infty \equiv \omega / c_\infty$ and the phase of $\sqrt{k_1^2 + k_3^2 - k_\infty^2}$ is equal to $-(i\pi/2)H(k_\infty^2 - k_1^2 - k_3^2)$, where H denotes the Heaviside function, it follows from (6.15) that

$$\mathcal{R}(y_2; \bar{x}, \omega) \rightarrow \frac{1}{2\pi i} \int_{-\infty}^{\infty} \int_{-\infty}^{\infty} e^{i|\bar{x}|h(k_1, k_3)} \Phi_{>/<}(k_1, k_3, y_2, \omega) \bar{G}(y_2 | 0; k_3, \omega / U(y_2), \omega) dk_3 dk_1 \quad (6.19)$$

as $|\bar{x}|, x_2 \rightarrow \pm\infty$, where

$$\Phi_{>/<}(k_1, k_3, y_2, \omega) \equiv \frac{\kappa_-(k_1, k_3, \omega) [k_1 U_s H(x_2) / \omega - 1]^2}{\kappa_+(\omega / U(y_2), k_3, \omega) [\omega / U(y_2) - k_1]} \frac{A_{>/<}(k_1, k_3, \omega)}{\hat{P}'_{>/<}(0; k_1, k_3, \omega)}, \quad (6.20)$$

$$\frac{A_<(k_1, k_3, \omega)}{\hat{P}'_<(0; k_1, k_3, \omega)} = \frac{1}{\sqrt{k_1^2 + k_3^2 - k_\infty^2}} \quad (6.21)$$

$$h \equiv k_1 \cos \theta + i \sqrt{k_1^2 + k_3^2 - k_\infty^2} \sin \theta \sin \psi + k_2 \sin \theta \cos \psi, \quad (6.22)$$

$|\bar{x}|^2 \equiv x_1^2 + x_2^2 + (x_3 - y_3)^2$, $\bar{x} = |\bar{x}| \{\cos \theta, \sin \theta \sin \psi, \sin \theta \cos \psi\}$ and we have put

$$\bar{G}(y_2 | 0; k_3, \omega / U(y_2), \omega) \equiv \frac{\omega^2 \hat{P}_>(y_2; \omega, \omega / U(y_2), k_3) (U_s / U(y_2) - 1)^2}{(2\pi)^3 c_s^2 \hat{P}'_>(0; \omega, \omega / U(y_2), k_3)}. \quad (6.23)$$

The integral in (6.19) can be evaluated by sequentially applying stationary phase to show that

$$\mathcal{R}(\bar{x}; y_2, \omega) \rightarrow - \frac{k_\infty \sin \theta \sin \psi}{|\bar{x}|} e^{i|\bar{x}|k_\infty} \Phi_{>/<}(k_1^{(s)}, k_3^{(s)}, y_2, \omega) \bar{G}(y_2 | 0; k_3^{(s)}, \omega / U(y_2), \omega), \quad (6.24)$$

as $|\bar{x}|, x_2 \rightarrow \pm\infty$, where $|\bar{x}|^2 \equiv x_1^2 + x_2^2 + x_3^2$,

$$k_3^{(s)} = k_\infty \sin \theta \cos \psi, \quad k_1^{(s)} = k_\infty \cos \theta. \quad (6.25)$$

Then since $|\bar{\mathbf{x}}| \sim |\mathbf{x}| - x_3 y_3 / |\mathbf{x}| = |\mathbf{x}| - y_3 \sin \theta \cos \psi$, it follows from (6.14) and (6.25) that the far field acoustic spectrum

$$\frac{1}{2\pi} \int_{-\infty}^{\infty} e^{i\omega\tau} p^s(\mathbf{x}, t) p^s(\mathbf{x}, t + \tau) d\tau = \lim_{T \rightarrow \infty} \overline{p^s(\mathbf{x}; \omega)} \left[\overline{p^s(\mathbf{x}; \omega)} \right]^* / 2T \quad (6.26)$$

is given in terms of the source spectrum (5.5) by

$$\begin{aligned} \frac{1}{2\pi} \int_{-\infty}^{\infty} e^{i\omega\tau} p^s(\mathbf{x}, t) p^s(\mathbf{x}, t + \tau) d\tau &= \left(\frac{(2\pi)^2 k_\infty \sin \theta \sin \psi}{|\mathbf{x}|} \right)^2 \int_0^\infty \int_0^\infty \Phi_{>/<} \left(k_1^{(s)}, k_3^{(s)}, y_2, \omega \right) \\ &\times \Phi_{>/<}^* \left(k_1^{(s)}, k_3^{(s)}, \tilde{y}_2, \omega \right) \bar{G} \left(y_2 | 0 : k_3^{(s)}, \omega / U(y_2), \omega \right) \bar{G}^* \left(\tilde{y}_2 | 0 : k_3^{(s)}, \omega / U(\tilde{y}_2), \omega \right) \\ &\times S \left(y_2, \tilde{y}_2 : k_3^{(s)}, \omega \right) dy_2 d\tilde{y}_2 \quad \text{for } x_2 > / < 0. \end{aligned} \quad (6.27)$$

The source function $S(y_2, \tilde{y}_2 : k_3^{(s)}, \omega)$ must, as indicated above, be modeled in terms of experimentally measurable turbulence statistics. Details are given sections 4 and 5. In order to evaluate the remaining factors in this formula it is necessary to first determine the homogeneous solutions $\hat{P}_>(y_2 : \omega, k_1, k_3)$, $\hat{P}_<(y_2 : \omega, k_1, k_3)$ of (A.3). These solutions can then be inserted into (6.13) and the (multiplicative) factorization can be carried out to determine κ_+ and κ_- . The results are used in (6.18), (6.20) and (6.23) to determine $\Phi_{>/<}$ and \bar{G} appearing in (6.27). These homogeneous solutions and, therefore, the subsequent factorization must be obtained numerically for $O(1)$ frequencies and general mean velocity profiles. The Wiener Hopf factorization (6.13) can be performed, for example, by using a procedure, such as the one given in Peake (2004) and Veitch & Peake (2008), to evaluate the integrals in the general factorization formula given in Noble (1958) numerically.

6.3 Low frequency limit

Since the experiments show that the radiated sound generated by the turbulent jet/trailing edge interaction is of relatively low frequency and since our focus here is on illustrating the general approach we simplify the computation of these factors by considering the asymptotic limit where $k_1, k_3 = O(k_\infty)$, $k_\infty \ll 1$. (This approximation is only made to simplify the computation of the Green's function and related quantities and will not be used when modeling S). The details are given in Appendix C, where it is shown that

$$\frac{\hat{P}_>(y_2 : \omega, k_1, k_3)}{\hat{P}'_>(0 : \omega, k_1, k_3)} = - \frac{1}{(k_1 U_s / \omega - 1)^2 \sqrt{k_1^2 + k_3^2 - k_\infty^2}} + O(1), \quad (6.28)$$

where $U_s = U(0)$ and

$$\kappa_+ \left(k_1, k_3^{(s)} \right) / \kappa_- \left(k_1, k_3^{(s)} \right) = \Gamma_0 \left(\omega, k_1, k_3^{(s)} \right) = - \frac{2}{\sqrt{k_1^2 - k_\infty^2 (1 - \sin^2 \theta \cos^2 \psi)}} + O(1), \quad (6.29)$$

Causality considerations (Briggs, 1964 and Bers, 1975) then require that

$$\kappa_- \left(k_1, k_3^{(s)} \right) = - \frac{\sqrt{k_1^2 - k_\infty^2 (1 - \sin^2 \theta \cos^2 \psi)}^{1/2}}{2} + \dots, \quad \kappa_+ \left(k_1, k_3^{(s)} \right) = \frac{1}{\sqrt{k_1^2 - k_\infty^2 (1 - \sin^2 \theta \cos^2 \psi)}^{1/2}} + \dots, \quad (6.30)$$

where the branch cuts are chosen so that $\arg \sqrt{k_1^2 - (k_\infty^2 - k_3^2)} = -\pi H(k_\infty^2 - k_1^2 - k_3^2)$.

Equations (B.1), (B.9), (B.12) can be combined with (6.4), (6.10), (6.28) and (6.30) to show that

$$\bar{G}(\mathbf{y}_T | \mathbf{x} : \omega, k_1) \sim \bar{G}^{(s)}(\mathbf{y}_T | \mathbf{x} : \omega, k_1) \sim k_1^{-3/2}, \quad \text{as } k_1 \rightarrow \infty, \quad (6.31)$$

and it then follows from Abel's theorem and equation (3.6) that

$$\bar{g}(\mathbf{y} | \mathbf{x} : \omega) \sim y_1^{1/2}, \quad \text{as } y_1 \rightarrow 0, \quad (6.32)$$

which means that the reduced Green's function $\bar{G}(\mathbf{y}_T | \mathbf{x} : \omega, k_1)$ that appears in the first line of equation (3.1) satisfies a Kutta condition at the trailing edge of the plate. Since the vortex sheet instability waves have zero growth rate and become purely convected disturbances in the low frequency limit, the causality condition implied by the factorization (6.29) insures that they are automatically included in the solution.

Substituting the low frequency results (6.28)-(6.30) into (6.20), (6.23) and (6.27) and using (6.10) and (B.1) shows that the far field acoustic spectrum is now given by the following relatively simple formula

$$I_\omega(\mathbf{x}) \equiv \frac{1}{2\pi} \int_{-\infty}^{\infty} e^{i\omega\tau} p^s(\mathbf{x}, t) p^s(\mathbf{x}, t + \tau) d\tau = \left(\frac{k_\infty}{4\pi|\mathbf{x}|} \right)^2 \int_0^\infty \int_0^\infty \frac{[M(y_2)M(\tilde{y}_2)]^{3/2}}{[1 - M(y_2)\cos\theta]} \\ \times \frac{(\beta - \cos\theta)S(y_2, \tilde{y}_2 : k_3^{(s)}, \omega)}{[1 - M(\tilde{y}_2)\cos\theta]\sqrt{[1 - \beta M(y_2)][1 - \beta M(\tilde{y}_2)]}} dy_2 d\tilde{y}_2, \quad (6.33)$$

where

$$\beta \equiv (1 - \sin^2 \theta \cos^2 \psi)^{1/2}, \quad (6.34)$$

$M(y_2) = U(y_2)/c_\infty$ denotes the local acoustic Mach number at the position y_2 and $k_3^{(s)}$ is given by (6.25). As noted above, this result is based on low-frequency asymptotics and may not completely describe all of the physical processes involved in the trailing edge interaction. It should, however, describe the experimentally observed low-frequency noise augmentation generated by this interaction

and does have the advantage of being much more explicit than the exact $O(1)$ frequency result(6.27). It can therefore provide some insight into the physics that it does describe. For example, its integrand can be interpreted as the product of the source function S with the directivity factor

$$\frac{[M(y_2)M(\tilde{y}_2)]^{3/2}(\beta - \cos \theta)}{[1 - M(y_2)\cos \theta][1 - M(\tilde{y}_2)\cos \theta]\sqrt{[1 - \beta M(y_2)][1 - \beta M(\tilde{y}_2)]}},$$

which is independent of the surface velocity U_s , is symmetric about the plane of the plate where $\psi = 0, \pi$, and causes the sound field to vanish in that plane. This result is proportional to $(1 - \cos \theta)/[1 - M(y_2)\cos \theta][1 - M(\tilde{y}_2)\cos \theta]$ in the plane perpendicular to the plate where $\psi = \pm\pi$ (since $\beta = 1$ there). As expected, it reproduces the directivity found by Ffowcs-Williams Hall (1970) when $M(y_2) = 0$, i.e. in the absence of a mean flow (see their equation 14) and, therefore, implies that the directivity peaks at 90 degrees for low subsonic Mach numbers.

We again suppose that the mean velocity profile and the mean sound speed profile are symmetric about the point $y_2 = y_d$ and choose $x_2^{(1)}$ and $x_2^{(2)}$ such that $U(x_2^{(2)}) = U(x_2^{(1)})$. The surface velocity must then vanish and it follows from (C.8) that the determinant of the matrix in equation (4.15) is now equal to zero (i.e. the matrix is singular) at lowest order of approximation since $H(x_2 - y_2)H(y_2 - x_2) = 0$. This means that the equation cannot be solved for $\hat{\Omega}$ unless $[\hat{V}_\perp^{(0)}(x_2^{(1)}, y_2, \omega, k_3), \hat{V}_\perp^{(0)}(x_2^{(2)}, y_2, \omega, k_3)]$ satisfies appropriate solvability conditions which, as noted above, implies that only one of the $\hat{V}_\perp^{(0)}(x_2^{(1)}, y_2, \omega, k_3), \hat{V}_\perp^{(0)}(x_2^{(2)}, y_2, \omega, k_3)$ can be specified independently and that there will be some arbitrariness in the choice of $\hat{\Omega}$. The lowest order matrix equation (4.15) also does not provide a uniformly valid approximation to $[\hat{V}_\perp^{(0)}(x_2^{(1)}, y_2, \omega, k_3), \hat{V}_\perp^{(0)}(x_2^{(2)}, y_2, \omega, k_3)]$ since, as noted in Appendix C, the $O(k_\infty)$ term in (C.8) can become smaller than the $O(k_\infty^2)$ term in the vicinity of the critical layer. These difficulties do not occur when the $O(k_\infty^2)$ terms are retained in this latter equation. The upper equation in the matrix (4.15) then becomes

$$\hat{V}_\perp^{(0)}(y_d, y_2, \omega, k_3) = -\frac{U^2(y_2)}{\omega|U'(y_2)|} \frac{k_\infty^2}{\sqrt{k_1^2 + k_3^2 - k_\infty^2}} \frac{[k_1 U(y_d) - \omega]}{ic^2(y_d)} \times$$

$$\left\{ \left[\frac{\sqrt{k_1^2 + k_3^2 - k_\infty^2} - y_d(k_1^2 + k_3^2 - k_\infty^2)}{k_\infty^2} + (k_1^2 + k_3^2) \int_{y_d}^{\infty} \left\{ \frac{c^2(\tilde{y})}{[k_1 U(\tilde{y}) - \omega]^2} - \frac{1}{k_\infty^2} \right\} d\tilde{y} \right] \hat{\Omega}(y_2; \omega, k_3) \right\}$$

$$+ \left[y_d - (k_1^2 + k_3^2) \int_0^{y_d} \frac{c^2(\tilde{y})}{[k_1 U(\tilde{y}) - \omega]^2} d\tilde{y} \right] \hat{\Omega}(2y_d - y_2 : \omega, k_3) \Bigg\}, \text{ for } y_2 \leq y_d, \quad (6.35)$$

with $k_1 = \omega / U(y_2)$ when the measurement point x_2 is set equal to y_d and the insignificant $O(k_\infty^2)$ terms are neglected in the coefficient. Then since

$$\frac{y_d}{k_\infty^2} + \int_{y_d}^{\infty} \left\{ \frac{c^2(\tilde{y})}{[k_1 U(\tilde{y}) - \omega]^2} - \frac{1}{k_\infty^2} \right\} d\tilde{y} = \int_0^{y_d} \frac{c^2(\tilde{y})}{[k_1 U(\tilde{y}) - \omega]^2} d\tilde{y}, \quad (6.36)$$

when $\omega / k_1 = U(y_2)$ and ω is assumed to have a small imaginary part in order to avoid the secondary singularity discussed in the paragraph following equation(4.15) (which occurs at y_2 in the first integral and at $2y_d - y_2$ in the second), this equation can be written more compactly by dividing $\hat{\Omega}(y_2 : \omega, k_3)$ into its even and odd symmetry components

$$\hat{\Omega}(y_2 : \omega, k_3) = A((y_2 - y_d)^2 : \omega, k_3) + (y_2 - y_d) B((y_2 - y_d)^2 : \omega, k_3) \quad (6.37)$$

to obtain

$$\begin{aligned} \hat{V}_\perp^{(0)}(y_d, y_2, \omega, k_3) = & - \frac{U^2(y_2)}{\omega |U'(y_2)|} \frac{k_\infty^2}{\sqrt{k_1^2 + k_3^2 - k_\infty^2}} \frac{[k_1 U(y_d) - \omega]}{ic^2(y_d)} \left\{ \frac{\sqrt{k_1^2 + k_3^2 - k_\infty^2} - 2y_d(k_1^2 + k_3^2 - k_\infty^2)}{k_\infty^2} [A - |y_2 - y_d|B] \right. \\ & \left. - 2(k_1^2 + k_3^2) \left[\int_0^{y_d} \frac{c^2(\tilde{y})}{[k_1 U(\tilde{y}) - \omega]^2} d\tilde{y} \right] |y_2 - y_d|B + 2y_d |y_2 - y_d|B \right\}, \end{aligned} \quad (6.38)$$

which can be further simplified by omitting higher order terms that don't play a role in making the approximation uniformly valid. To this end we suppose, for definiteness, that $c^2 = \text{constant}$, $U(y_2)$ is zero for $|y_2 - y_d| \geq t_d/2$ and is given by

$$U(y_2) = U_J(y_2) = U_d \left\{ 1 - [2(y_2 - y_d)/t_d]^2 \right\}, \text{ for } |y_2 - y_d| \leq t_d/2, \quad (6.39)$$

with $t_d \leq 2y_d$ being the jet thickness. (see comment below (C.8)). Then since

$$\int_{y_d - t_d/2}^{y_d} \frac{c^2(\tilde{y})}{[k_1 U(\tilde{y}) - \omega]^2} d\tilde{y} = \frac{c^2(y_d) U^2(y_2) (t_d/2)^4}{U_d^2 \omega^2} \int_{y_d - t_d/2}^{y_d} \frac{1}{[(\tilde{y} - y_d)^2 - (y_2 - y_d)^2]^2} d\tilde{y} =$$

$$-\frac{c^2(y_d)U^2(y_2)(t_d/2)^4}{2U_d^2\omega^2(y_2-y_d)^2}\left\{\frac{(t_d/2)}{(t_d/2)^2-(y_2-y_d)^2}+\frac{1}{2|y_2-y_d|}\left[\ln\left(\frac{(t_d/2)-|y_2-y_d|}{(t_d/2)+|y_2-y_d|}\right)+i\pi\right]\right\}, \quad (6.40)$$

where, as noted above, the second critical layer singularity is avoided by assuming that $k_1 = \omega/U(y_2)$ and, therefore, $(y_2 - y_d)$ has a small imaginary part which is set to zero after the integration is carried out (also see remarks below (C.7)).

Since the real part of (6.40) remains bounded when $y_2 \rightarrow y_d$ (due to cancellation between the \ln term and the first term in curly brackets), the lowest order uniformly valid approximation to equation (6.38) is given by

$$\hat{V}_\perp^{(0)}(y_d, y_2, \omega, k_3) \approx -\frac{U(y_2)}{i|U'(y_2)|}\left\{\frac{[U(y_d)-U(y_2)]}{c^2(y_d)}(A-|y_2-y_d|B)+\frac{k_\infty^2(k_1^2+k_3^2)}{\sqrt{k_1^2+k_3^2-k_\infty^2}}\frac{i\pi U^2(y_2)}{\omega^2 U''}B\right\}, \quad (6.41)$$

and since the contribution from (6.40) is formally independent of the assumed velocity profile (6.39) it is expected to be quite generic. However, it cannot by itself be used to determine the two quantities A and B and, therefore, $\hat{\Omega}(y_2 : \omega, k_3)$. But since our purpose here is to obtain a simple result that illustrates the general procedure, we set $B = b_0 A / y_d$ (where b_0 is an adjustable positive constant) to obtain

$$\begin{aligned} \hat{V}_\perp^{(0)}(y_d, y_2, \omega, k_3) \approx & -\frac{U(y_2)}{i|U'(y_2)|}\left\{\left[\frac{[U(y_d)-U(y_2)]}{c^2(y_d)}\left(1-\frac{|y_2-y_d|}{y_d}b_0\right)\right.\right. \\ & \left.\left.+\frac{k_\infty^2(k_1^2+k_3^2)}{\sqrt{k_1^2+k_3^2-k_\infty^2}}\frac{i\pi U^2(y_2)b_0}{\omega^2 U'' y_d}\right]\frac{\hat{\Omega}(y_2 : \omega, k_3)}{\left(1+\frac{y_2-y_d}{y_d}b_0\right)}\right\}. \end{aligned} \quad (6.42)$$

Inserting this into (5.5) and (5.6) leads to the relatively simple relation

$$S(y_2, \tilde{y}_2 : k_3, \omega) = \frac{|U'(y_2)U'(\tilde{y}_2)|\left(1+\frac{y_2-y_d}{y_d}b_0\right)\left(1+\frac{\tilde{y}_2-y_d}{y_d}b_0\right)F_\perp(y_d, y_d|y_2, \tilde{y}_2, \omega, k_3)}{[U(y_2)U(\tilde{y}_2)]E(y_2 : k_3, \omega)[E(\tilde{y}_2 : k_3, \omega)]^*} \quad (6.43)$$

between S and $F_\perp(y_d, y_d|y_2, \tilde{y}_2, \omega, k_3)$ where

$$E(y_2 : k_3, \omega) \equiv \frac{[U(y_d)-U(y_2)]\left(1-\frac{|y_2-y_d|}{y_d}b_0\right)}{c^2(y_d)}+\frac{\left[\omega^2/U^2(y_2)+k_3^2\right]}{\sqrt{\omega^2/U^2(y_2)+k_3^2-k_\infty^2}}\frac{i\pi U^2(y_2)b_0}{c_\infty^2 U'' y_d}. \quad (6.44)$$

We use this as the working formula for relating S to the measurable statistics.

6.4 Source Model

The spectrum $F_{\perp}(y_d, y_d | y_2, \tilde{y}_2, \omega, k_3)$, which is related to the cross correlation (5.9) of the transverse velocity fluctuations by (5.8) and (5.10), needs be specified before this result can actually be used. This quantity has been extensively measured and the data is well documented in the literature. These results are well represented by a model of the type (Leib & Goldstein, 2011)

$$\langle \rho v'_{\perp}(x_1, y_d, x_3, t) \rho v'_{\perp}(\tilde{x}_1, y_d, x_3 + \eta_3, t + \tau) \rangle = L_3 \Psi(\bar{x}_1) e^{-\sqrt{(\eta_1/l_1)^2 + [(\eta_1 - U_c \tau)/l_0]^2 + (\eta_3/l_3)^2}}, \quad (6.45)$$

where $\eta_1 \equiv \tilde{x}_1 - x_1$ and $\bar{x}_1 \equiv (x_1 + \tilde{x}_1)/2$.

While we expect this quantity to be independent of the streamwise coordinate for the nearly parallel flow being envisioned here, we initially allow Ψ to decay in the streamwise direction in order to insure convergence of the integrals in (5.10). Then it seems reasonable to set

$$\Psi(\bar{x}_1) = \Psi_0 e^{-(\bar{x}_1/L_1)^2}, \quad (6.46)$$

where Ψ_0 is expected to scale with the transverse component of the mean square turbulence momentum flux $(\rho v'_{\perp})^2$, L_1, L_3 are constants, with L_3 being a measure of the transverse extent of the turbulence and the specific choice of L_1 , which is expected to be large in order to insure that the correlation (6.45) is relatively independent of \bar{x}_1 , will be specified in the next subsection.

Inserting this into (5.8)-(5.10) shows that

$$F_{\perp}(x_2, x_2 | y_2, \tilde{y}_2, \omega, k_3) = \left(\frac{L_3 l_0 l_1 l_3 \Psi_0}{2\pi^2 U_c} \right) \frac{L_1 e^{-[L_1(k_1 - \tilde{k}_1)/2]^2}}{[(\omega l_0/U_c)^2 + \chi]^2}, \quad (6.47)$$

where $k_1 = \omega/U(y_2)$, $\tilde{k}_1 = \omega/U(\tilde{y}_2)$ and

$$\chi = \chi(U(\tilde{y}_2), U(y_2)) = \left[(k_3 l_3)^2 + (k_1/2 + \tilde{k}_1/2 - \omega/U_c)^2 l_1^2 + 1 \right]. \quad (6.48)$$

6.5 Final formula

Inserting (6.43) and (6.47) into equation (6.33) and appropriately accounting for the symmetry about $y_2 = y_d$ shows that

$$I_{\omega}(\mathbf{x}) = \left(\frac{1}{4\pi|\mathbf{x}|} \right)^2 \left(\frac{k_{\infty} l_0 l_1 l_3 L_3 \Psi_0}{\pi^{3/2} U_c c_{\infty}} \right) (\beta - \cos \theta) I_0(Ma, \theta, \psi) \quad (6.49)$$

where β is given by (6.34),

$$I_0(Ma, \theta, \psi) \equiv 4 \int_0^{U(y_d)} \int_0^{U(y_d)} \frac{[M(y_2)M(\tilde{y}_2)]^{3/2}}{[1 - M(y_2)\cos\theta][1 - M(\tilde{y}_2)\cos\theta]\sqrt{[1 - \beta M(\tilde{y}_2)]}U(y_2)U(\tilde{y}_2)}$$

$$\times \frac{\left\{ \omega L_1 e^{-[L_1(k_1 - \tilde{k}_1)/2]^2} / 2\sqrt{\pi} \right\} dU(y_2) dU(\tilde{y}_2)}{\sqrt{[1 - \beta M(y_2)]} E(y_2 : k_3^{(s)}, \omega) \left[E(\tilde{y}_2 : k_3^{(s)}, \omega) \right]^* \left[(\omega l_0 / U_c)^2 + \chi(U(y_2), U(\tilde{y}_2)) \right]^2}, \quad (6.50)$$

with E is defined by(6.44), $k_3^{(s)}$ is given by(6.25) and

$$Ma \equiv U(y_d) / c_\infty \quad (6.51)$$

denotes the maximum acoustic Mach number.

As noted in the previous subsection, our interest is in the case where L_1 is large and the experimental turbulence correlation (6.45) becomes independent of the streamwise coordinate x_1 . Then since

(Lighthill, 1964, p.17) $L_1 e^{-[L_1(k_1 - \tilde{k}_1)/2]^2} \rightarrow 2\sqrt{\pi} \delta(k_1 - \tilde{k}_1)$ as $L_1 \rightarrow \infty$ and

$\omega \delta(k_1 - \tilde{k}_1) / U^2(y_2) = \delta(U(y_2) - U(\tilde{y}_2))$, it follows that

$$I_0 \rightarrow 4 \int_0^{Ma} \frac{c_\infty M^3 dM}{(1 - M \cos \theta)^2 (1 - \beta M) \left| E(y_2 : k_3^{(s)}, \omega) \right|^2 \left[(\omega l_0 / U_c)^2 + \chi(M) \right]^2}, \quad (6.52)$$

where we have put

$$\chi(M) \equiv \chi(U(y_2), U(y_2)). \quad (6.53)$$

Since Ψ_0 scales with the velocity squared and it can be shown that $I_0 \sim 1/\omega$ as $\omega \rightarrow 0$, this result implies that the acoustic spectrum should scale with the 4th power of velocity, which is consistent with the 5th power of velocity scaling for the overall sound power level found by Ffowcs-Williams and Hall (1970) when Strouhal number scaling is assumed.

6.6 Numerical results and discussion

The acoustic spectrum produced by the planar jet /trailing edge interaction can be computed by inserting (6.52), with E given by (6.44), into(6.49), which was obtained by inserting the approximate formula (6.43) for S into(6.33). The exact result, which is given by the much less explicit formula (6.27) is currently being computed (see Afsar, Goldstein & Leib,2013) but, for purposes of illustration, the approximate equation (6.49) was used to obtain figure 4, which shows some typical results for the normalized far-field pressure spectrum $10 \log \left[I_\omega / (\rho_s^2 c_\infty^2 D U_d) \right]$ plotted against Strouhal number for a range of peak acoustic Mach numbers, Ma . The mean density ρ is assumed to be constant and for calculational purposes we approximate the symmetric mean velocity profile $U(y_2) = U_J(y_2)$ by

$$U(y_2) = U_d \left[e^{-\alpha^2(y_2 - y_d)^2} - e^{-\alpha^2(t_d/2)^2} \right] / \left[1 - e^{-\alpha^2(t_d/2)^2} \right] \quad (6.54)$$

over the range $|y_2 - y_d| \leq t_d / 2$ and set $(\alpha D)^2 = 2.3$ (where D is defined more precisely below) in order to fit the mean flow measurements of Zaman, Brown and Bridges (2013).

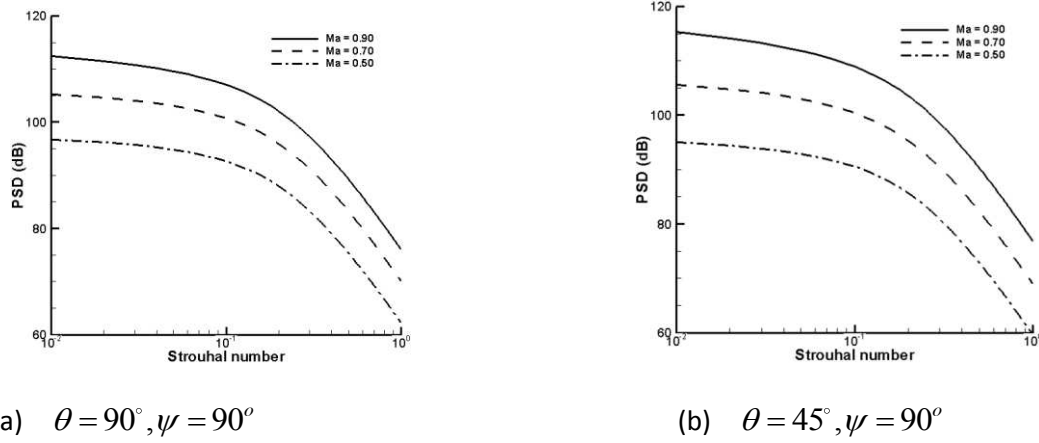


Figure 4. RDT trends with Ma . Trailing edge at $y_d/D = 1.2, x_d/D = 5.7$ Source model constants are $\Psi_0 = 0.04(\rho_\infty U_d)^2, l_0/D = 0.45, l_1/D = 0.01, l_3/D = 0.01, L_2 = 0.5D, L_3 = 2.5D, t_d = 2.2, U_c = 0.68U_d, b_0 = 0.4, |x|/D = 100$, and $D = 2.12''$. a) $\theta = 90^\circ, \psi = 90^\circ$, (b), $\theta = 45^\circ, \psi = 90^\circ$.

Figure 4, which is in qualitative agreement with experimental observations *over the frequency range where amplification occurs*, shows that the peak noise levels occur at fairly low Strouhal numbers and increase with increasing Ma . There is relatively little polar directivity, but the highest levels occur at ninety degrees to the jet axis at low Mach numbers (as predicted by Ffowcs Williams and Hall, 1970) and at smaller angles (around 45°) at higher Mach numbers. Equation (6.33) shows that the radiated sound field is symmetric about the plane of the plate—suggesting a dipole-like behavior—but the two Doppler factors in the denominator are reminiscent of a moving monopole type source.

As stated earlier, the model problem considered in this section can be used to represent the interaction between a jet emanating from a large-aspect ratio rectangular nozzle with the trailing edge of a flat plate. Recent experiments on this configuration were performed at NASA Glenn Research Center (Zaman, Brown and Bridges 2013; Bridges and Brown, 2013). The relevant geometric parameters are shown in figure 5.

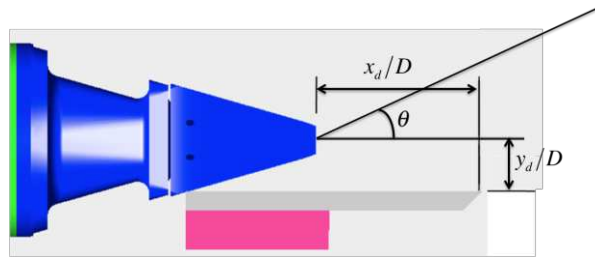


Figure 5 Nozzle/plate configuration. Figure courtesy Dr. James E. Bridges, NASA Glenn.

Figures 6 and 7 are quantitative comparisons of the far-field pressure fluctuations' power spectral density per unit Strouhal number, in dB scale, $PSD \equiv 10 \log(4\pi I_\omega U_d / D p_{ref}^2)$ (referenced to $p_{ref} = 20 \mu pa$), computed from the low frequency RDT result (6.49) with the acoustic data of

Bridges and Brown (2013), taken in an anechoic facility validated for jet noise measurements (Bridges & Brown 2005; Brown & Bridges 2006). The arbitrary length scale D is now taken to be an equivalent nozzle diameter defined by $\pi(D/2)^2 = \text{nozzle width} \times \text{nozzle height}$ with nozzle width = 8 × nozzle height and $\approx 2.12''$ in the Brown & Bridges (2006) experiments. The plate trailing edge was located at 1.2 equivalent diameters from the jet centerline and 5.7 equivalent diameters downstream of the nozzle exit in the case selected for these comparisons. Any 'scrubbing noise' that may have resulted from the flow along the plate was deemed to be negligible in this case (see Zaman, Brown and Bridges, 2013).

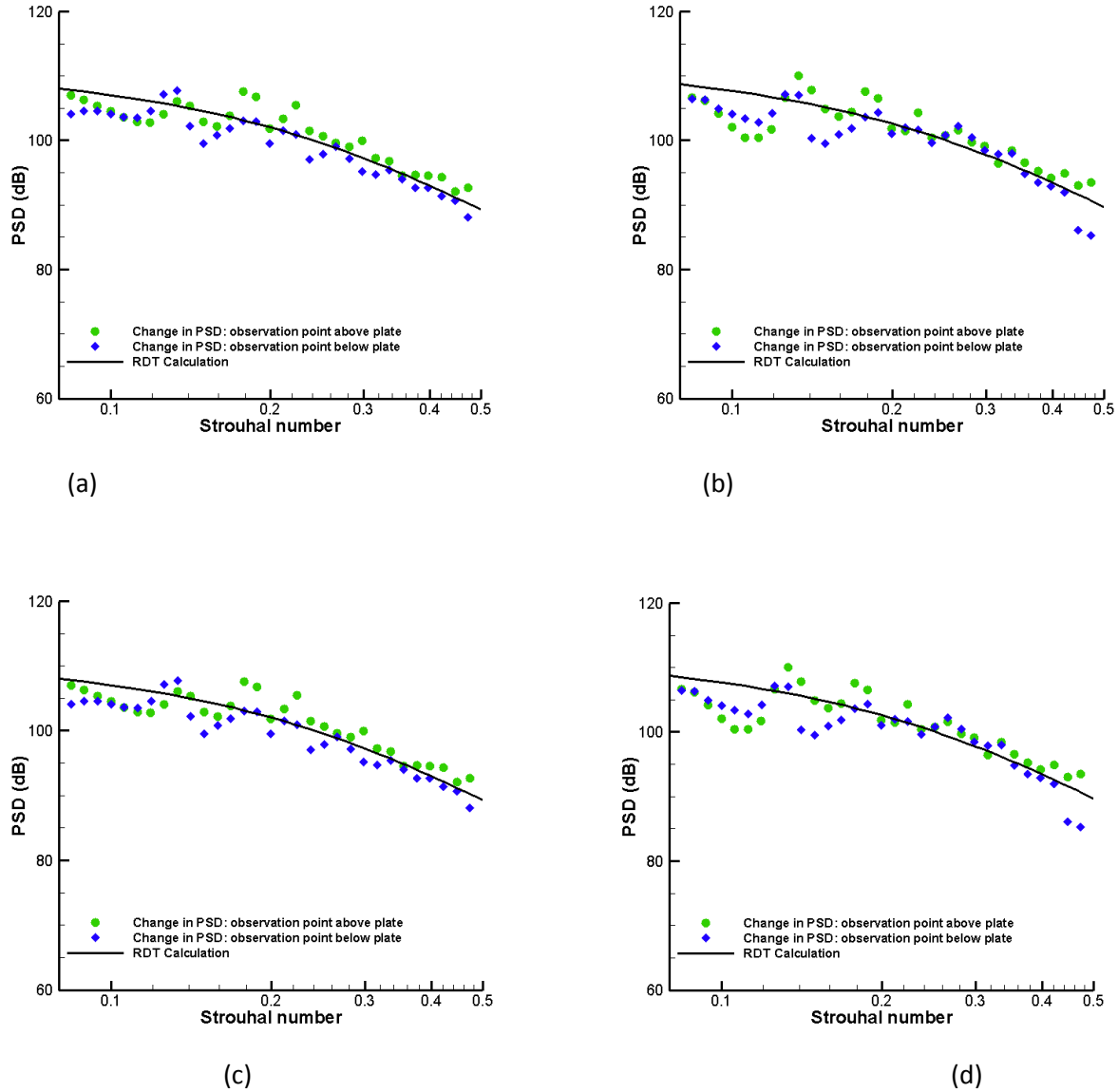


Figure 6 Predicted (curves) and measured (green/blue symbols above/below the plate) Power Spectral Density (PSD) of the far-field pressure fluctuations at 100 equivalent diameters from nozzle exit (lossless in dB scale referenced to $20 \mu \text{Pa}$) as a function of Strouhal number, for $Ma = 0.9$. Plate trailing edge at $y_d/D = 1.2, x_d/D = 5.7, D = 2.12'', U_c = 0.62U_d, \psi = \pm 90^\circ$. Source model constants are the same as in figure 4. a) $\theta = 90^\circ$; (b) $\theta = 75^\circ$; (c) $\theta = 60^\circ$; (d) $\theta = 45^\circ$

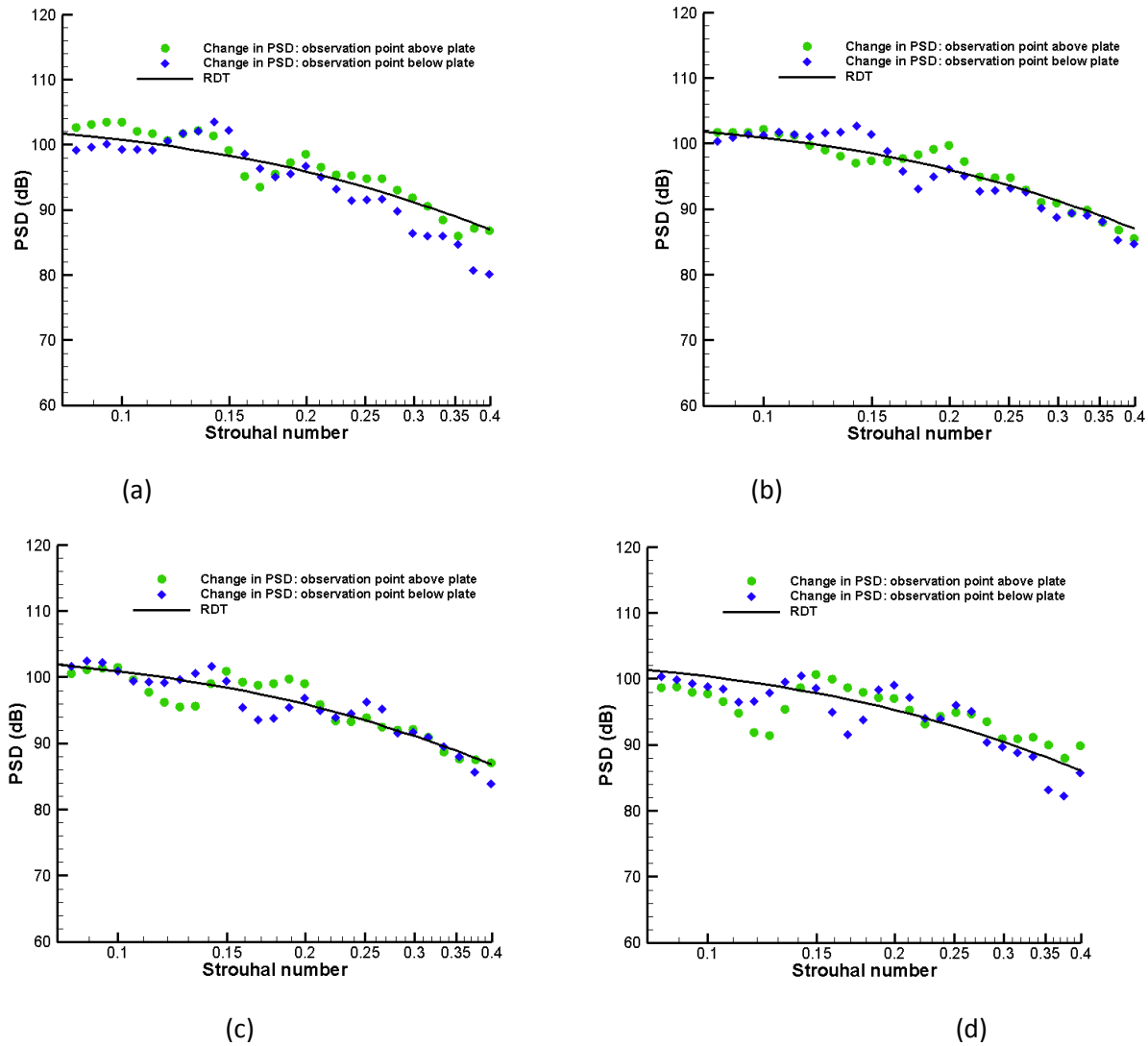


Figure 7 Predicted (curves) and measured (green/blue symbols above/below the plate) Power Spectral Density (PSD) of the far-field pressure fluctuations at 100 equivalent diameters from nozzle exit (lossless in dB scale referenced to $20 \mu \text{Pa}$) as a function of Strouhal number, for $Ma = 0.7$. Plate trailing edge at $y_d/D = 1.2, x_d/D = 5.7, U_c = 0.5U_d, \psi = \pm 90^\circ, D = 2.12''$. Source model constants are the same as in figure 4. a) $\theta = 90^\circ$; (b) $\theta = 75^\circ$; (c) $\theta = 60^\circ$; (d) $\theta = 45^\circ$.

Comparisons are presented for two jet exit acoustic Mach numbers, Ma , of 0.7 and 0.9, four polar angles measure from the downstream jet axis $\theta = 90^\circ, 75^\circ, 60^\circ, 45^\circ$ and two azimuthal angles, corresponding to observer locations above and below the plate ($\psi = \pm 90^\circ$). The trailing edge noise is extracted from the total acoustic spectrum by subtracting out the noise from a free jet measured in the same facility. The Strouhal numbers in these comparisons are restricted to a range where there is significant amplification over the corresponding free jet noise. The source model parameters used in the calculations are the same as those in figure 4.

The results show that the RDT based predictions are in good quantitative agreement with the data. The theory indicates that the sound radiated above the plate is the same as that below (i.e. dipole-like

directivity) which is also observed (to within experimental uncertainty) in the data. The agreement is best at ninety degrees (parts (a) of the figures), where the low Mach number edge-generated noise is predicted to be maximal (see eqns.(6.49) and(6.52)). But the agreement is still reasonable at forty-five degrees, even though the edge-generated noise is difficult to isolate from the pure jet noise (Bridges and Brown, 2013). Oscillations appear around a Strouhal number of 0.1 for all cases, suggesting that a feedback-generated tone may be occurring in the experiment (Zaman, Brown and Bridges (2013), Bridges and Brown, 2013).

7. Concluding remarks

This paper is based on the formal solutions (2.18) and (2.27) to the linearized Euler equations for transversely sheared mean flows which, like the Kovaszny results for the unsteady motion on uniform flows, involve two arbitrary convected quantities $\mathfrak{G}(\tau - y_1 / U, \mathbf{y}_T)$ and $\tilde{\omega}_c(\tau - y_1 / U, \mathbf{y}_T)$ that can be associated with the hydrodynamic component of the flow and can, therefore, be used to specify upstream boundary (i.e. initial) conditions for RDT problems that involve the interaction of turbulence with solid surfaces. But, unlike the Kovaszny result, these quantities do not bear a simple relation to the physically measurable variables that can be controlled by the experimentalist. A method for determining these relations is, therefore, developed in sections 4 and 5. The results are used to relate the statistical quantities that are the main output of RDT to physically measurable statistical quantities that are independent of the streamwise coordinate. The general solutions (2.18) and (2.27) relating the unsteady flow to these convected quantities therefore provide a natural way of inputting the upstream boundary conditions into streamwise inhomogeneous RDT problems.

The results derived in this paper were used to extend Non-homogeneous Rapid Distortion Theory to transversely sheared base flows. The extended theory can be used to obtain solutions to turbulence-surface interaction problems that include the effects of rotational mean flows. An example of the type of problems to which the theory can be applied is given in Section 6. It shows how the results developed in this paper can be used to predict noise generated by the interaction of a two-dimensional jet with a semi-infinite flat plate – a problem of significant current interest. The exact results are valid for all (i.e., $O(1)$) frequencies, but low frequency asymptotics were used to obtain specific formulas that have the advantage of being much more explicit than the $O(1)$ frequency results and can, therefore, provide some insight into the physics that they describe.

The formalism can, of course, be applied to many other RDT problems involving the interaction of turbulence with surfaces embedded in transversely sheared base flows or, more generally, in vortical base flows that asymptote to transversely sheared mean flows in the upstream region.

Acknowledgement

The authors would like to thank Drs. Khairul Zaman, James Bridges and Clifford Brown for providing their experimental data and their helpful comments. They would also like to thank Miss Daria Frank (Ph.D. candidate, Department of Applied Mathematics and Theoretical Physics, Cambridge, UK) for her excellent translation of the Möhring paper. MZA would like to thank the NASA Post-doctoral Program

(NPP) for financial support (NPP liaison, Dr. David Kankam). This work was also supported by the NASA fundamental Aeronautics Program's High-Speed and Fixed Wing Projects.

Appendix A. Green's function for 2-D base flow

The reduced Green's function

$$\hat{G}(y_2 | x_2 : \omega, k_1, \hat{k}) \equiv \frac{1}{2\pi} \int_{-\infty}^{\infty} e^{i(y_3 - x_3)\hat{k}} \bar{G}(y_T | x_T : \omega, k_1) d(y_3 - x_3) \quad (\text{A.1})$$

for the planar mean flow

$$U = U(y_2), \quad c = c(y_2) \quad (\text{A.2})$$

satisfies the reduced Rayleigh equation

$$\frac{d}{dy_2} \left\{ \frac{c^2(y_2)}{[\omega - U(y_2)k_1]^2} \frac{d\hat{G}}{dy_2} \right\} + \left\{ 1 - \frac{c^2(y_2)}{[\omega - U(y_2)k_1]^2} (k_1^2 + k_3^2) \right\} \hat{G} = \frac{\delta(x_2 - y_2)}{(2\pi)^3}, \quad (\text{A.3})$$

whose solution is given by

$$\hat{G}(x_2 | y_2) = \hat{G}(y_2 | x_2) = \frac{\hat{P}_+(y_2)\hat{P}_-(x_2)}{\Delta(k_1, k_3, \omega)} \quad \text{for } y_2 > / < x_2, \quad (\text{A.4})$$

where $\hat{P}_+(y_2), \hat{P}_-(y_2)$ are the homogeneous solutions of (A.3) that exhibit appropriate boundary conditions at the outer/inner edges of the shear layer and, according to Abel's theorem,

$$\Delta(\omega, k_1, k_3) \equiv - \frac{(2\pi)^3 c^2 [\hat{P}_+(y_2)\hat{P}'_-(y_2) - \hat{P}'_+(y_2)\hat{P}_-(y_2)]}{[\omega - U(y_2)k_1]^2} \quad (\text{A.5})$$

depends on the normalization of $\hat{P}_+(y_2), \hat{P}_-(y_2)$ but is independent of y_2 . So the limit

$$\lim_{k_1 \rightarrow \omega/U(y_2)} \Delta(k_1, k_3, \omega) \quad (\text{A.6})$$

is expected to exist and be non-zero except at perhaps at a finite number of points, say $y_2 = y_2^{(n)}(\omega)$, for $n = 1, 2, \dots$ for any value of k_3, ω . Moreover it follows from the method of Frobenius that (A.3) possesses two linearly independent solutions, say $\hat{P}_1(y_2), \hat{P}_2(y_2)$, that behave like

$$\hat{P}_1(y_2) = O\left((\omega - k_1 U(y_2))^3\right) = O\left((y_2 - y_2^{(0)})^3\right), \quad (\text{A.7})$$

$$\hat{P}_2(y_2) = a + b\hat{P}_1(y_2) \ln(\omega - k_1 U(y_2)) + O(\omega - k_1 U(y_2)), \quad (\text{A.8})$$

as $y_2 \rightarrow y_2^{(0)}$, where $y_2^{(0)}$ is a point where $U(y_2^{(0)}) = \omega / k_1$ and a, b are normalization constants. So

$$\lim_{\substack{k_1 \rightarrow \omega/U(y_2) \\ y_2 = \text{const.}}} \left\{ \hat{P}_+(y_2 : k_1, k_3, \omega), \hat{P}_-(y_2 : k_1, k_3, \omega) \right\} =$$

$$\lim_{\substack{y_2 \rightarrow y_2^{(0)} \\ y_2^{(0)} = \text{const.}}} \left\{ \hat{P}_+(y_2 : \omega/U(y_2^{(0)}), k_3, \omega), \hat{P}_-(y_2 : \omega/U(y_2^{(0)}), k_3, \omega) \right\} \quad (\text{A.9})$$

is also expected to exist and be non-zero since $\hat{P}_+(y_2), \hat{P}_-(y_2)$ must be linear combinations of $\hat{P}_1(y_2), \hat{P}_2(y_2)$. It, therefore, follows from (A.1) and (A.4) that the limit (3.5) also exists and is non-zero everywhere except at the finite number of points where Δ is equal to zero. But since $\Delta(\omega, k_1, k_3) = 0$ is the dispersion relation for the linear instability waves these points will correspond to the neutral wave numbers, say, $k_1^N = \omega/U(y_2^N)$ which must lie on the critical layer at some transverse position $y_2 = y_2^N$.

For example Squire's theorem shows that the neutral instability point will occur at a fixed value of ω/k_1 and $k_1^2 + k_3^2$ when the flow is incompressible. A singular point, is, therefore, expected to occur at a fixed value of ω for each value of k_3 .

Appendix B Solution to The Wiener Hopf problem

Equation (6.6) and (6.7) imply that

$$H_+(x_1, x_2 : k_1, k_2) = \frac{\hat{G}'_>(0 | x_1, x_2 : \omega, k_1, k_3)}{(k_1 U_s / \omega - 1)^2} = \hat{G}'_<(0 | x_1, x_2 : \omega, k_1, k_3), \quad (\text{B.1})$$

where the \pm subscripts now denote analytic functions in the upper/lower half k_1 -plane, and it follows from equations (6.8) and (6.10) that

$$\text{sgn}(x_2) \int_{-\infty}^{\infty} e^{ik_1(x_1 - y_1)} \hat{G}^{(0)}(0 | x_2 : \omega, k_1, k_3) dk_1$$

$$+ \int_{-\infty}^{\infty} e^{-ik_1 y_1} \hat{G}'_>(0 | x_1, x_2 : \omega, k_1, k_3) (k_1 U_s / \omega - 1)^{-2} \Gamma_0(\omega, k_1, k_3) dk_1 = 0, \text{ for } y_1 > 0, \quad (\text{B.2})$$

where $\Gamma_0(\omega, k_1, k_3)$, which is defined in (6.13), satisfies (6.13) and is, therefore, independent of the solutions $\hat{G}'_{>,<}(0 | x_1, x_2 : \omega, k_1, k_3)$ to the Wiener Hopf problem (6.6)-(6.8). Inserting

$$F_+(x_1, x_2 : k_1, k_3) + F_-(x_1, x_2 : k_1, k_3) \equiv \frac{\hat{G}'_>(0 | x_1, x_2 : \omega, k_1, k_3)}{(k_1 U_s / \omega - 1)^2} \Gamma_0(\omega, k_1, k_3)$$

$$= H_+(x_1, x_2 : k_1, k_2) \Gamma_0(\omega, k_1, k_3) \quad (\text{B.3})$$

into (B.2) shows that

$$F_+(x_1, x_2 : k_1, k_3) \equiv -\frac{1}{2\pi} \int_0^\infty \int_{-\infty}^\infty e^{-i(\tilde{k}_1 - k_1)y_1} e^{i\tilde{k}_1 x_1} \text{sgn}(x_2) \hat{G}^{(0)}(0 | x_1, x_2 : \omega, \tilde{k}_1, k_3) d\tilde{k}_1 dy_1 =$$

$$-\frac{1}{2\pi i} \int_{-\infty}^\infty \frac{e^{i\tilde{k}_1 x_1} \text{sgn}(x_2) \hat{G}^{(0)}(0 | x_2 : \omega, \tilde{k}_1, k_3)}{\tilde{k}_1 - k_1} d\tilde{k}_1, \quad (\text{B.4})$$

which implies that

$$H_+(x_1, x_2 : k_1, k_3) \kappa_+(k_1, k_3) - \kappa_-(k_1, k_3) F_-(x_1, x_2 : k_1, k_3) = \kappa_-(k_1, k_3) F_+(x_1, x_2 : k_1, k_3) \quad (\text{B.5})$$

when $\Gamma_0(k_1, k_3)$ is factored as

$$\kappa_+(k_1, k_3) / \kappa_-(k_1, k_3) = \Gamma_0(\omega, k_1, k_3). \quad (\text{B.6})$$

It then follows that

$$J_+(x_1, x_2 : k_1, k_3) - H_+(x_1, x_2 : k_1, k_3) \kappa_+(k_1, k_3) =$$

$$J_-(x_1, x_2 : k_1, k_3) - \kappa_-(k_1, k_3) F_-(x_1, x_2 : k_1, k_3) = E, \quad (\text{B.7})$$

where $E(x_1, x_2, k_1, k_3)$ is an entire function of k_1 and $J_\pm(x_1, x_2 : k_1, k_3)$ satisfies the jump condition

$$J_+(x_1, x_2 : k_1, k_3) - J_-(x_1, x_2 : k_1, k_3) = \kappa_-(k_1, k_3) F_+(x_1, x_2 : k_1, k_3) \quad (\text{B.8})$$

Since $\kappa_+(k_1, k_3) \sim k_1^{-1/2}$ as $k_1 \rightarrow \infty$ while equation (B.12) below shows that $J_+ \sim 1/k_1$ as $k_1 \rightarrow \infty$ equations (B.1), (6.10), together with Liouville's theorem show that the solution

$\hat{G}_{>/<}(y_2 | x_1, x_2 : \omega, k_1, k_3)$ will only decay as $k_1 \rightarrow \infty$ when the entire function $E(x_1, x_2, k_1, k_3)$ is set equal to zero, which as usual, produces the minimum edge singularity at $y_1 = 0$. We, therefore, set

$$J_+(x_1, x_2 : k_1, k_3) = H_+(x_1, x_2 : k_1, k_3) \kappa_+(k_1, k_3). \quad (\text{B.9})$$

But applying the Plemelj formulas (Woods 1961) to (B.4) shows that

$$F_+(x_1, x_2 : k_1, k_3; \omega) - F_-(x_1, x_2 : k_1, k_3; \omega) = -\text{sgn}(x_2) e^{i\tilde{k}_1 x_1} \hat{G}^{(0)}(0 | x_2 : \omega, k_1, k_3), \quad (\text{B.10})$$

where $F_-(x_1, x_2 : k_1, k_3; \omega)$ is an analytic function in the lower half k_1 plane which is bounded at infinity.

Inserting this into (B.8) shows that

$$K_-(x_1, x_2 : k_1, k_3; \omega) - J_+(x_1, x_2 : k_1, k_3; \omega) = \kappa_-(k_1, k_3) \text{sgn}(x_2) e^{i\tilde{k}_1 x_1} \hat{G}_0(0 | x_2 : k_1, k_3, \omega), \quad (\text{B.11})$$

where $K_-(x_1, x_2 : k_1, k_3; \omega) \equiv J_-(x_1, x_2 : k_1, k_3; \omega) + F_-(x_1, x_2 : k_1, k_3; \omega) \kappa_-(k_1, k_3; \omega)$ is an analytic function in the lower half k_1 -plane with analytic behavior at infinity. Applying the Plemelj formulas to this result yields

$$J_+(x_1, x_2 : k_1, k_3; \omega) = -\frac{1}{2\pi i} \lim_{\delta \rightarrow +0} \int_{-\infty}^{\infty} \frac{\kappa_- (\tilde{k}, k_3) \operatorname{sgn}(x_2) e^{i\tilde{k}x_1} \hat{G}^{(0)}(0 | x_2 : \tilde{k}, k_3, \omega)}{\tilde{k} - k_1 - i\delta} d\tilde{k}. \quad (\text{B.12})$$

It, therefore, follows from (6.1)-(6.4), (B.1), (6.10) and (B.9) that the solution for the Fourier transformed pressure $\hat{p}'(x_1, x_2 : \omega, k_3)$ is given by equations (6.11) and (6.12).

Appendix C Low frequency limit

In this Appendix we consider the asymptotic limit where $k_1, k_3 = O(k_\infty)$, $k_\infty \ll 1$ and suppose that $x_2, y_2 \geq 0$. Then the relevant homogeneous solutions to equation (A.3) are given by

$$\hat{P}_+(y_2 : k_1, k_3) = \hat{P}_>(y_2 : k_1, k_3) = A_> \exp(-\sqrt{k_1^2 + k_3^2 - k_\infty^2} y_2), \quad (\text{C.1})$$

$$\hat{P}_-(y_2 : k_1, k_3) = A_- \exp(-\sqrt{k_1^2 + k_3^2 - k_\infty^2} y_2) + B_- \exp(\sqrt{k_1^2 + k_3^2 - k_\infty^2} y_2) \quad (\text{C.2})$$

in the outer region where $k_\infty y_2 = O(1)$ and by

$$\hat{P}_>(y_2 : k_1, k_3) = A_> \left\| 1 - \frac{\sqrt{k_1^2 + k_3^2 - k_\infty^2}}{k_\infty^2} \left\{ k_\infty^2 y_2 - \int_{y_2}^{\infty} \left[\frac{(k_1 U - \omega)^2}{c^2} - k_\infty^2 \right] d\tilde{y} \right\} \right\| + O(k_\infty^2), \quad (\text{C.3})$$

$$\hat{P}_-(y_2 : k_1, k_3) = (A_- + B_-) - (A_- - B_-) \frac{\sqrt{k_1^2 + k_3^2 - k_\infty^2}}{k_\infty^2} \left\{ k_\infty^2 y_2 - \int_{y_2}^{\infty} \left[\frac{(k_1 U - \omega)^2}{c^2} - k_\infty^2 \right] d\tilde{y} \right\} \quad (\text{C.4})$$

in the inner region where $y_2 = O(1)$. The inner boundary condition (6.5) on

$\hat{G}^{(0)}(y_2 | x_2 : \omega, k_1, k_3)$ implies that $A_- = B_-$ in equation (C.7) and it follows that

$$\hat{P}_-(y_2 : k_1, k_3) = 2A_- + O(k_\infty^2) \quad \text{for } y_2 = O(1). \quad (\text{C.5})$$

Equation (A.3), therefore implies that

$$\begin{aligned} \hat{P}'_>(y_2 : k_1, k_3) = & -A_> \frac{[k_1 U(y_2) - \omega]^2}{c^2(y_2)} \left\| \frac{\sqrt{k_1^2 + k_3^2 - k_\infty^2}}{k_\infty^2} - y_2 \frac{(k_1^2 + k_3^2 - k_\infty^2)}{k_\infty^2} \right. \\ & \left. + (k_1^2 + k_3^2) \int_{y_2}^{\infty} \left\{ \frac{c^2(\tilde{y})}{[k_1 U(\tilde{y}) - \omega]^2} - \frac{1}{k_\infty^2} \right\} d\tilde{y} \right\| + O(k_\infty^3) \quad \text{for } y_2 = O(1) \end{aligned} \quad (\text{C.6})$$

and

$$\hat{P}'_-(y_2) = -2A_- \frac{[k_1 U(y_2) - \omega]^2}{c^2(y_2)} \int_0^{y_2} \left\{ 1 - \frac{c^2(\tilde{y})(k_1^2 + k_3^2)}{[k_1 U(\tilde{y}) - \omega]^2} \right\} d\tilde{y} + O(k_\infty^3) \text{ for } y_2 = O(1), \quad (\text{C.7})$$

where, as explained in the paragraph following equation (4.15) the relevant solution is obtained by assuming that ω has a small imaginary part when ω/k_1 is set equal U in order to avoid the second critical layer singularity that would otherwise occur at the symmetrically located point $2y_d - y_2$ (since $U(y_2) = U(2y_d - y_2)$). It now follows that $\Gamma_0(\omega, k_1, k_3^*)$ and $\hat{P}'_>(y_2 : \omega, \omega/U(y_2), k_3)/\hat{P}'_>(0 : \omega, \omega/U(y_2), k_3)$ are given by equations (6.28) and (6.29) respectively.

It also follows from (C.6) together with equations (3.11), (4.13), (6.16), (C.3), (C.4), (A.4) and (B.5) of Goldstein et al, (2013) (see comment below equation (4.6)), that the transverse velocity Green's function $\hat{G}_2^{(0)}(y_2 | x_2 : \omega, \omega/U(y_2), k_3)$, which appears in equation (4.10), is given by

$$\begin{aligned} \hat{G}_2^{(0)}(y_2 | x_2) = & \left[\frac{k_\infty^2}{(2\pi)^3 \sqrt{k_1^2 + k_3^2 - k_\infty^2}} + O(k_\infty^2) \right] \frac{[k_1 U(x_2) - \omega]}{ic^2(x_2)} \times \\ & \left\{ \left\| x_2 - (k_1^2 + k_3^2) \int_0^{x_2} \frac{c^2(\tilde{y})}{[k_1 U(\tilde{y}) - \omega]^2} d\tilde{y} \right\| H(y_2 - x_2) + \left\| \frac{\sqrt{k_1^2 + k_3^2 - k_\infty^2}}{k_\infty^2} - x_2 \frac{(k_1^2 + k_3^2 - k_\infty^2)}{k_\infty^2} \right. \right. \\ & \left. \left. + (k_1^2 + k_3^2) \int_{x_2}^\infty \left\{ \frac{c^2(\tilde{y})}{[k_1 U(\tilde{y}) - \omega]^2} - \frac{1}{k_\infty^2} \right\} d\tilde{y} \right\| H(x_2 - y_2) \right\} \quad (\text{C.8}) \end{aligned}$$

to within an $O(k_\infty^3)$ error. This result applies even when the shear layer has finite width and U' is, therefore, discontinuous at some points. Notice that the lowest order term in this equation vanishes at the critical level where $y_2 = x_2$ while the higher order terms do not, which means that the lowest order approximation is not uniformly valid in y_2, x_2 . But integrating by parts and comparing the result with the local Frobenius solution shows that the two term expansion has the correct critical layer behavior and therefore provides a uniformly valid result.

References

- Afsar, M. Z., Goldstein, M. E. & Leib, S. J. 2013. Prediction of trailing edge noise using Rapid Distortion Theory. European Turbulence Conference (ETC 14). ENS Lyon, Lyon, France, 1st-3rd September 2013.
- Bers, A. 1975 Linear waves and instabilities. *In Plasma Physics* (eds. C. Dewitt & J. Perraud), pp. 113-216. Gordon & Breach.
- Bridges, J. and Brown, C.A. "Validation of the small hot jet rig for jet noise research," AIAA Paper 2005-2846, 2005.

- Bridges, J. and Brown, C.A. 2013 Jet \ surface interaction tests: Acoustic Measurements. In preparation
- Briggs, R. J. 1964 *Electron Stream Interaction with Plasmas*. MIT Press
- Brown, C. , 2012 "Jet-Surface Interaction Test: Far-Field Noise Results", ASME Paper GT2012-69639.
- Brown, C.A. and Bridges, J., 2006, Small hot jet acoustic rig validation, NASA-TM-2006-214234.
- Crighton, D. G. & Leppington, F. G., 1970, Scattering of aerodynamic noise by a semi-infinite compliant plate. J. Fluid Mech. 43 (40 721-736
- Dowling, A. P., Ffowcs Williams J. E. & Goldstein, M. E. 1978, Sound propagation in a moving stream, Phil. Trans. R. Soc. London, A288 pp321-34940, 657-670
- Drazin, P. G., Reid, W. H., 1981, Hydrodynamic Stability, Cambridge University Press, Cambridge UK
- Ffowcs Williams, J. E. and Hall, L. H., 1970, Aerodynamic sound generation by turbulent flow in the vicinity of a scattering half plane, J. Fluid Mech., 40, 657-670
- Goldstein, M.E., 1978 a, Unsteady vortical and entropic distortions of potential flows round arbitrary obstacles, J. Fluid Mech. Vol.89, pp. 433-468
- Goldstein, M.E., 1978 b Characteristics of the unsteady motion on transversely sheared mean flows, J. Fluid Mech. Vol.84, part 2, pp. 305-329
- Goldstein, M.E., 1979 a Scattering and distortion of the unsteady motion on transversely sheared mean Flows, J. Fluid Mech. Vol. 91, pp. 601-632
- Goldstein, M.E., 1979 b, turbulence generated by entropy fluctuation with non-uniform mean flows, J. Fluid Mech. Vol. 93, part 2 pp. 209-224
- Goldstein, M.E., 2005, On Identifying the true sources of aerodynamic sound , J. Fluid Mech. Vol. 526, pp. 337-347
- Goldstein, M.E., 2009, A theoretical basis for identifying the sound sources in a turbulent flow, international journal of Aeroacoustics.Vol.8 no. 4, pp. 283-300
- Goldstein, M.E., Afsar, M. Z. and Leib, 2013, Structure of small amplitude motion on transversely sheared mean flows, NASA/TM—2103-217862
- Heaton, C. J. and Peake, N. 2006, Algebraic and exponential instability of inviscid swirling flow, J. Fluid Mech. Vol. 565, pp. 279-318
- Hunt, J. C. R. 1973 A theory of turbulent flow around two dimensional bluff bodies J. Fluid Mech. Vol. 61, pp. 625-706
- Hunt, J. C. R., 1977, A review of the theory of rapidly distorted flows and its application s. 13th Biennial Fluid Dyn. Symp., Poland

Hunt, J.C.R and Carruthers, D.J.,1990 Rapid distortion theory and the 'problems' of turbulence, J. Fluid Mech. Vol. 212, pp. 497-532.

Jaworski, J. W. & Peake, N. 2013 Aerodynamic noise from a poroelastic edge with implications for the silent flight of owls, J. Fluid Mech. Vol 723 pp. 456-479

Kovaszny, L. S. G., 1953, Turbulence in supersonic flow, J. Aero Sci. 20, issue number 10pp. 657-674.

Leib, S.J. and Goldstein, M.E., 2011 "Hybrid Source Model for Predicting High-Speed Jet Noise," *AIAA Journal*, Vol. 49, No. 7

Lighthill, M. J. 1964 Fourier Analysis and Generalized Functions, Cambridge University Press

Mani, R. 1976, Influence of jet flow on jet noise, *Journal of Fluid Mech.* 173 pp. 753-793

Möhring, W., 1976 Über Schallwellen in Scherströmungen, Fortschritte der Akustik. DAGA 76 VDI pp.543-546

Morse, P. M. and Feshbach, H., 1953, Methods of Theoretical Physics, McGraw-Hill Book Company

Noble, B. 1988 Methods Based on the Wiener Hopf Technique for the Solution of Partial Differential Equations Chelsea

Orr, W. (1907), The stability and instability of the steady motions of a perfect liquid and of a viscous liquid, Proc. Roy. Irish Acad., A 27, 9-68 and 69-138

Peake, N. 2004 On the unsteady motion of a long fluid-loaded elastic plate with mean flow, J. Fluid Mech. 507, 335–366

Sagaut, P. & Cambon, C., 2008, Homogeneous turbulence Dynamics, Cambridge University press, Cambridge U.K

Sears, W.R., 1941, Some aspects of non-stationary airfoil theory and its practical application, J. Aero. Sci. vol. 83, p. 104

Tam, C. K.W. & Auriault, L. 1998, mean flow refraction effects on sound radiated from localized sources in a jet, J. Fluid Mech. Vol. 370, pp. 149-174

Veitch, B. & Peake, N. 2008 Acoustic propagation and scattering in the exhaust flow from coaxial cylinders. J. Fluid Mech. 613, 275–307.

Woods, L.C. 1961, The Theory of Subsonic Plane Flow, Cambridge University Press.

Zaman, K.; Brown, C. A.; Bridges, J. E., 2013, Interaction of a Rectangular Jet with a Flat-plate placed parallel to the Flow AIAA-2013-2184.